AFOSR-TR- 91 0054

Final Report • November 1990

MULTIPHOTON DETECTION TECHNIQUES FOR F AND F_2

Gregory W. Faris, Mark J. Dyer,
William K. Bischel, and David L. Huestis
Molecular Physics Laboratory

SRI Project 6066
Contract No. F49620-88-K-0003
MP 90-141R

Prepared for:

Air Force Office of Scientific Research
Building 410
Bolling AFB, DC 20332-6448

Attn: Dr. Julian M. Tishkoff AFOSR/NA

Final Report • November 1990

MULTIPHOTON DETECTION TECHNIQUES FOR F AND F_2

Gregory W. Faris, Mark J. Dyer,
William K. Bischel, and David L. Huestis
Molecular Physics Laboratory

SRI Project 6066
Contract No. F49620-88-K-0003
MP 90-141R

Prepared for:

Air Force Office of Scientific Research
Building 410
Bolling AFB, DC 20332-6448

Attn: Dr. Julian M. Tishkoff AFOSR/NA

Approved:

Donald J. Eckstrom, Director
Molecular Physics Laboratory

G. R. Abrahamson
Senior Vice President
Sciences Group

SRI International 333 Ravenswood Avenue • Menlo Park, CA 94025-3493 • (415) 326-6200 • FAX (415) 326-5512 • Telex 334486

REPORT DOCUMENTATION PAGE

Form Approved OMB No. 0704-0188

1. AGENCY USE ONLY *(Leave blank)*	2. REPORT DATE	3. REPORT TYPE AND DATES COVERED
	901108	Final TAPC TR-91MAR-10

4. TITLE AND SUBTITLE
Multiphoton Detection Techniques for F and F2 (U)

5. FUNDING NUMBERS
PE - 61102F
PR - 2308
TA - A3
G - F-49620-88-K-0003

6. AUTHOR(S)
Faris, G. W.; Dyer, M. J.; Bischel, W. K.; Huestis, D. L.

7. PERFORMING ORGANIZATION NAME(S) AND ADDRESS(ES)
SRI International
333 Ravenswood Avenue
Menlo Park, CA 94025

8. PERFORMING ORGANIZATION REPORT NUMBER
MP 90-141

9. SPONSORING/MONITORING AGENCY NAME(S) AND ADDRESS(ES)
AFOSR/NA
Building 410
Bolling AFB, DC 20332-6448
Attn: Dr. Julian M. Tishkoff

10. SPONSORING/MONITORING AGENCY REPORT NUMBER

11. SUPPLEMENTARY NOTES

12a. DISTRIBUTION/AVAILABILITY STATEMENT
Approved for public release; distribution is unlimited

12b. DISTRIBUTION CODE

13. ABSTRACT *(Maximum 200 words)*

This report describes research toward the development of quantitative remote diagnostics for atomic and molecular fluorine, using ultraviolet multiphoton excitation followed by the detection of fluorescence or ionization. The first demonstration of resonant two-photon excitation of molecular fluorine is described, which allows sensitive detection of molecular fluorine. A high power uv-vuv laser source based on Raman-shifting a narrow-band, tunable excimer laser in liquid-nitrogen-cooled isotopes of hydrogen has been developed and applied to two-photon detection of both molecular and atomic fluorine.

14. SUBJECT TERMS
multiphoton detection, two-photon excited fluorescence, lasers, fluorine, ultraviolet sources, TPEF, F, F2.

15. NUMBER OF PAGES
54

16. PRICE CODE

17. SECURITY CLASSIFICATION OF REPORT	18. SECURITY CLASSIFICATION OF THIS PAGE	19. SECURITY CLASSIFICATION OF ABSTRACT	20. LIMITATION OF ABSTRACT
Unclassified	Unclassified	Unclassified	UL

CONTENTS

ILLUSTRATIONS

INTRODUCTION

The goal of this work was to develop quantitative detection techniques for F and F_2 based on multiphoton excitation of high-lying atomic or molecular states. Because of their high ionization potentials, F and F_2 are among the most difficult neutral chemical species to detect spectroscopically. Our research program included (1) development of the necessary high-power, narrow-band ultraviolet radiation sources, (2) identification and experimental observation of appropriate multiphoton transitions, and (3) study of the relevant spectroscopic parameters to establish reliable, quantitative detection techniques.

There are a number of possible optical detection techniques for F and F_2. For F, the possibilities include vuv absorption at 95 nm,[1] magnetic dipole absorption at 404 cm^{-1} in the ground state,[2-5] spontaneous or stimulated Raman spectroscopy on the ground state,[2] and two-[6] or three[7]-photon-resonant excited fluorescence or ionization. For F_2, the possibilities include continuum absorption at 280 nm,[8] spontaneous or stimulated Raman scattering on the ground state, and two-[9] or three[7]-photon-resonant excited fluorescence or ionization.

The desired characteristics for an optical detection technique include (1) good sensitivity, (2) high temporal and spatial resolution, (3) quantitative results, (4) *in situ* measurements with minimal perturbation to the system under study, and (5) minimal interferences and minimal sensitivity on ambient conditions. The Raman techniques can have good sensitivity and resolution, but because the signal is proportional to the population difference [or population difference squared for coherent anti-Stokes Raman scattering (CARS)], Raman measurements are temperature sensitive and quantitative concentration measurements are difficult to obtain. The 95-nm vuv absorption in F lies below the LiF window cutoff, so no windows are available to transmit the required light. The 404-cm^{-1} absorption in F and the 280-nm absorption in F_2 have low sensitivity, and unless tomographic techniques are used, the measurements represent only concentrations integrated along the light path. Two-photon resonantly-excited fluorescence can provide the positive characteristics of good sensitivity as well as good spatial and temporal resolution for quantitative, *in situ* measurements. Three-photon-resonant excitation schemes allow the use of longer laser wavelengths, but the cross sections are lower, and no fluorescence has been observed.[7]

In our studies of F_2, vibrational levels v' = 0, 1, 2, and 3 of the $F^1\Pi_g$ state and v' = 3 of the $f^3\Pi_g$ state have been excited from the ground $X^1\Sigma_g^+$ state by two photons near 207 nm and detected by vuv fluorescence or by ionization by a third photon. In addition to providing a means

of detecting the ground state concentration of F_2, the two-photon excitation scheme we have developed should be useful in investigating the kinetics of the 157-nm F_2 laser, which is believed to arise from a transition from the outer well of the $f^3\Pi_g$ state to a weakly bound $^3\Pi_u$ state.

To make practical the quantitative detection of atomic fluorine by two-photon excited fluorescence (TPEF) using a 170-nm pump laser, we had to develop a new laser source that is much more intense than the sixth-order anti-Stokes Raman shifted doubled dye laser we had used previously. Such a laser system has now been assembled, along with an appropriate experimental cell and detection equipment. It is based on using both a stronger ultraviolet primary laser (ArF) and lower order Raman shifting (only two shifts). With this laser source, detection of both F and F_2 has been demonstrated.

SUMMARY OF RESEARCH ACCOMPLISHMENTS

TWO-PHOTON SPECTROSCOPY OF THE $F^1\Pi_g$ AND $F^3\Pi_g$ STATES OF F_2

These results are covered in detail in the technical paper included as the Appendix. We have demonstrated a sensitive technique for the detection of F_2 based upon two-photon excitation followed by detection of vuv fluorescence or detection of ions created by absorption of a third photon. Both the $F^1\Pi_g$ and $f^3\Pi_g$ states have been excited. These are the first instances of two-photon-resonant excitation of F_2, and the $f^3\Pi_g$ spectra represent the first instances of two-photon singlet to triplet molecular excitation to our knowledge. An excitation spectrum for the $F^1\Pi_g$ state is shown in Figure 1. The excitation wavelengths were generated by doubling an excimer-pumped dye laser in a β-BaB_2O_4 crystal. Calibration of the laser wavelength was obtained by simultaneous recording of a 1+1 REMPI signal from the $B^2\Pi \leftarrow X^2\Pi$ (3,0) β band in NO, which was subsequently calibrated against iodine fluorescence. As shown in Figure 1, ion and fluorescence signals for the $F^1\Pi_g$ state agree very well with calculated spectra based upon two-photon Hönl-London factors.[10] The ion and fluorescence signals for the $f^3\Pi_g$ state agree fairly well with a theoretical spectrum that ignores the spin-orbit fine structure of the $f^3\Pi_g$ state. The vuv fluorescence was resolved with a vacuum monochromator. An emission spectrum, shown in Figure 2, demonstrates that the fluorescence occurs on the F_2 laser transition. This is the first optical pumping of the F_2 vuv laser transition. Power dependence of the fluorescence intensity and pressure dependence of the temporal profile of the fluorescence indicate that population of the upper state probably occurs through the creation of ions. In addition to providing a promising diagnostic for measuring F_2, two-photon excitation allows study of the F_2 laser transition with optical excitation.

GENERATION OF 170-nm AND 205-nm RADIATION BY RAMAN-SHIFTING AN ARF LASER IN HD AND D_2

A suitable detection scheme for atomic fluorine was demonstrated during the previous AFOSR contract (No. F49620-85-K-0005).[6,11] This scheme involves two-photon excitation with 170-nm light followed by detection of fluorescence at 776 nm, as is shown in Figure 3. In the previous experiments, the 170-nm light was generated by sixth-order anti-Stokes Raman shifting in H_2 of the 30-mJ output at 280 nm of a doubled Nd:YAG-pumped dye laser. The resulting laser energy at 170 nm was on the order of 10 μJ and the intensity fluctuations were large, yet the light

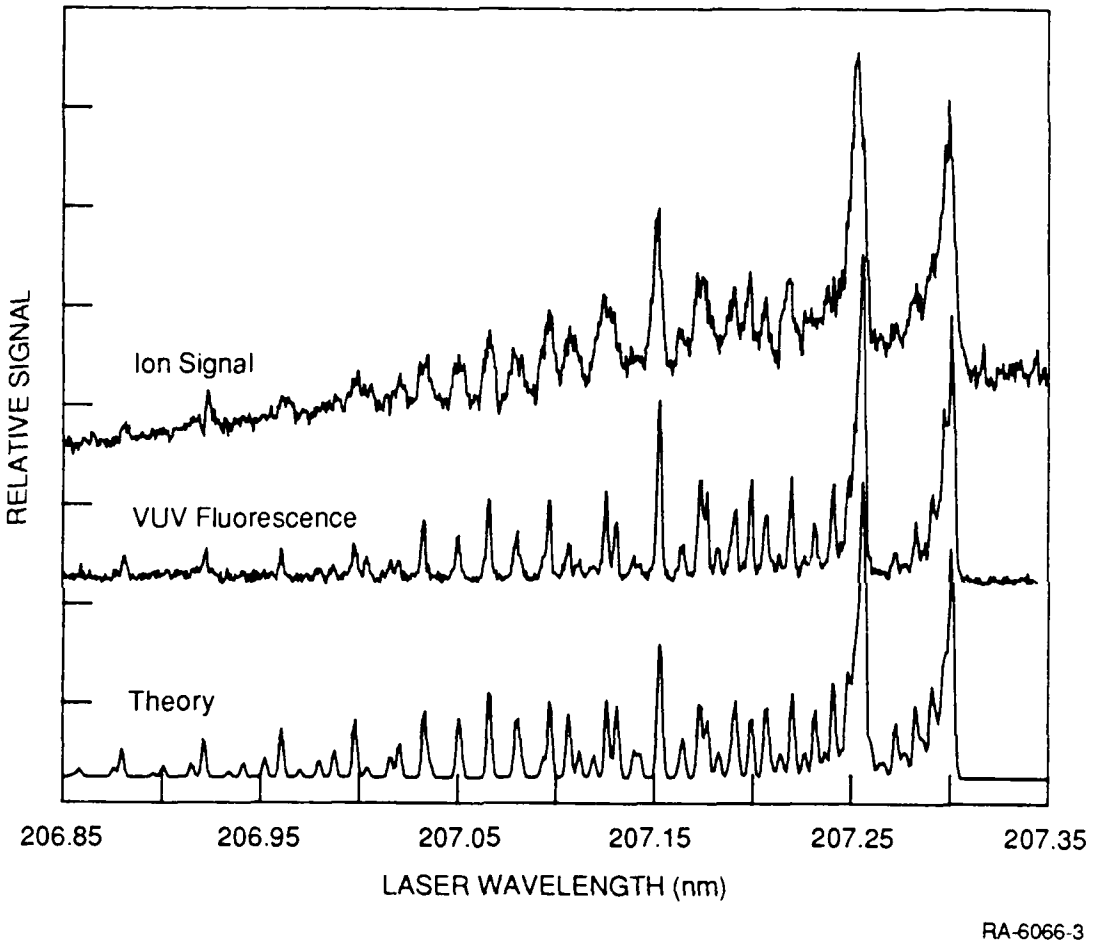

Figure 1. Two-photon excitation spectrum for the $F^1\Pi_g$ (v' = 2) ← $X^1\Pi_g^+$ (v" = 0) transition in F_2.

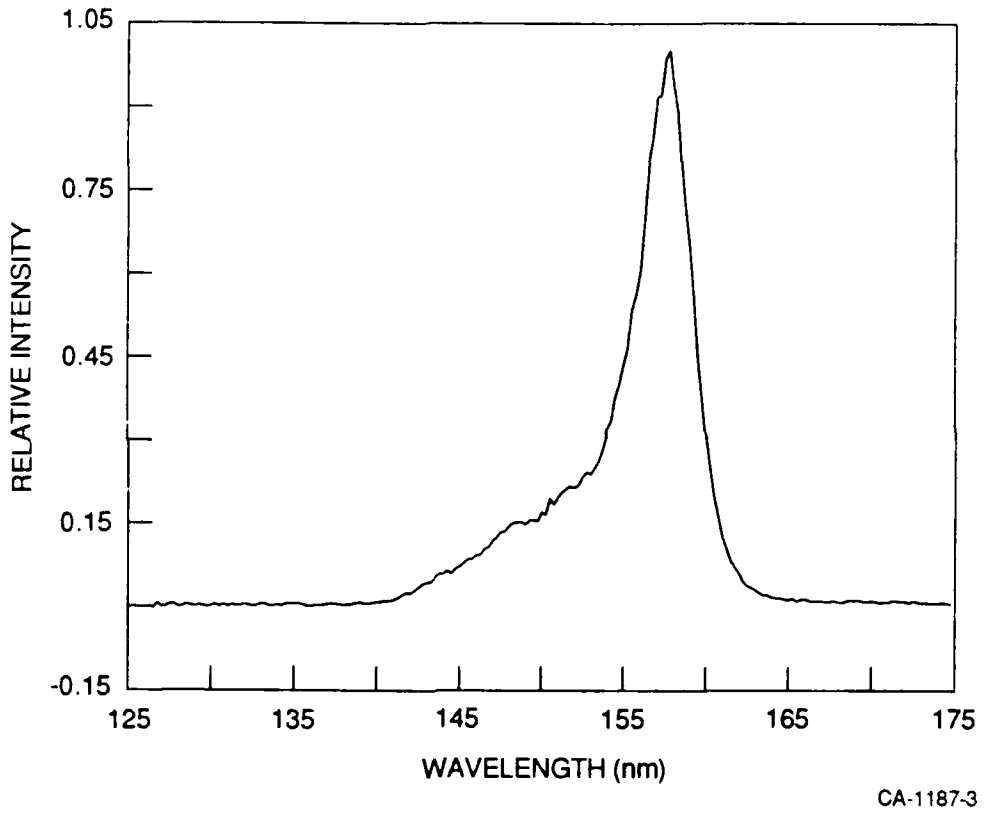

Figure 2. VUV emission spectrum for two-photon excitation of the $F^1\Pi_g$ (v' = 2) $\leftarrow X^1\Pi_g^+$ (v" = 0) transition in F_2.

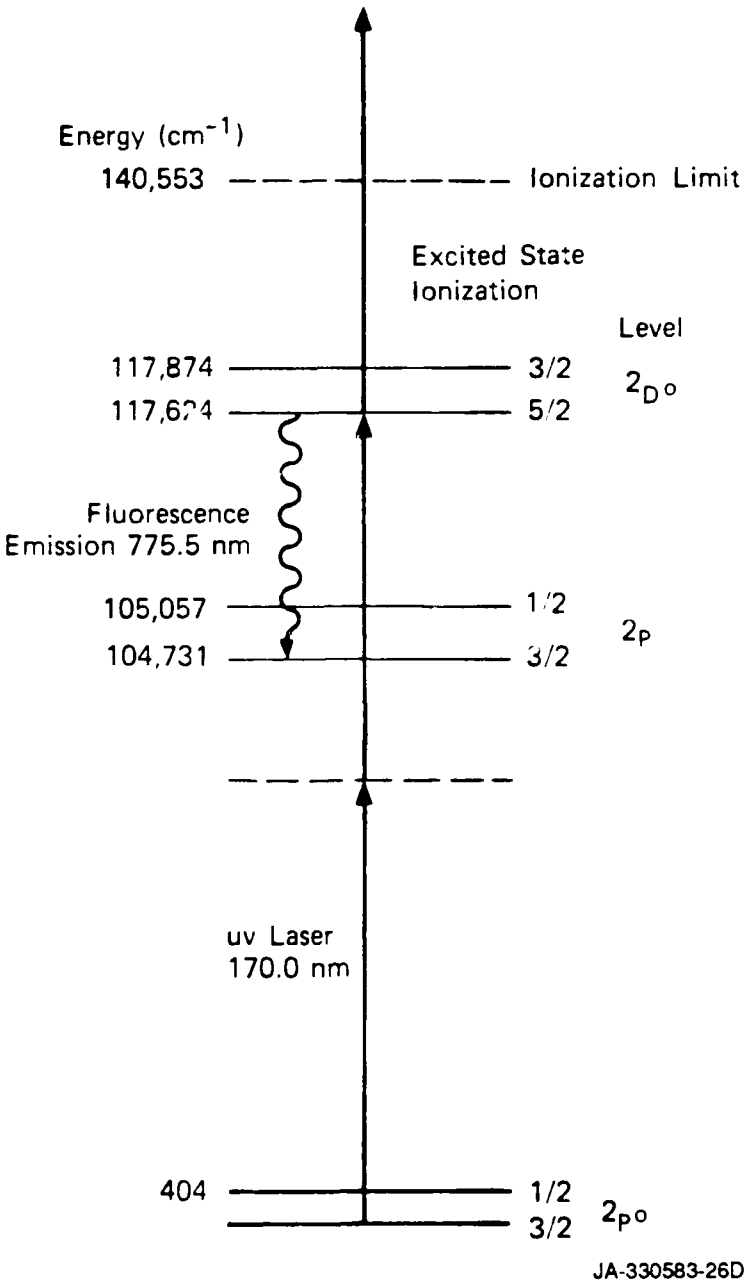

Figure 3. Excitation scheme for two-photon detection of F atoms.

source was sufficient to obtain signals with good signal to noise ratios. Three of the four fine structure components obtained for the $^2D^o \leftarrow {}^2P^o$ excitation are shown in Figure 4. Because the sensitivity of the detection technique depends on the square of the pump laser intensity, it is important to obtain as large an energy at 170 nm as possible. In addition, the intensity fluctuations should be small to allow accurate measurements.

We have developed a new approach for the production of higher powers for both F and F_2 detection. There is a coincidental overlap between the tuning range of the ArF excimer laser when the laser is twice anti-Stokes Raman-shifted in HD gas and the energy for two-photon excitation of the $^2D^o_{3/2} \leftarrow {}^2P^o_{3/2}$ fine structure line of atomic fluorine. Additionally, there are two-photon coincidences for the $F^1\Pi_g \leftarrow X^1\Sigma_g$ v' = 3 and v' = 2 transitions in molecular fluorine with the first Stokes Raman-shifted lines of ArF in D_2 and HD, respectively. The advantage of this approach is that the ArF laser is much closer to the desired wavelength and thus allows use of only second-order anti-Stokes Raman shiftingthereby allowing higher power and smaller intensity fluctuations (previous experience suggests at least a factor of three reduction in output for each anti-Stokes order, and intensity fluctuations that increase with each additional Raman shift). A technical problem we had to address is that the only gas with the appropriate Raman shift energy for F atom detection is HD, which under normal conditions has a smaller Raman gain and conversion efficiency than H_2 and D_2. The approach adopted to compensate for the lower conversion efficiency is to cool the HD Raman cell to the temperature of liquid nitrogen (77 K). This cooling increases the gain coefficient by redistribution of the HD ground state population, reduction of the Raman linewidth, and reduction of the losses as impurities are frozen out.

The apparatus for this scheme is shown in Figure 5. The laser used is a modified Lambda-Physik (150 MSC) oscillator-amplifier. The oscillator provides ~1.3 mJ energy in ~1 cm^{-1}, tunable over about 1 nm. When the laser was operated as a standard oscillator injection-locked amplifier pair, the spatial mode was of inadequate quality for multiple-order anti-Stokes Raman shifting. For this reason, a number of modifications were made to the laser. To improve the quality of the spatial mode input to the amplifier, the beam from the oscillator was passed through a spatial filter consisting of a pinhole and two curved mirrors. To reduce degradation of the mode quality in the amplifier, the amplifier's unstable resonator was removed, and mirrors were added to allow triple passing the amplifier discharge. The triple passing was done vertically to fill the vertically oriented aspect ratio of the amplifier discharge. The gas fill for the amplifier was adjusted to give a peak gain at a later time to compensate for the later arrival of the oscillator pulse in this arrangement. The MgF_2 windows on both the oscillator and amplifier discharges led to significant depolarization of the beam. The beam polarization was greatly improved by adjustment of the window orientation. The 193-nm radiation produced by Raman-shifting a frequency-

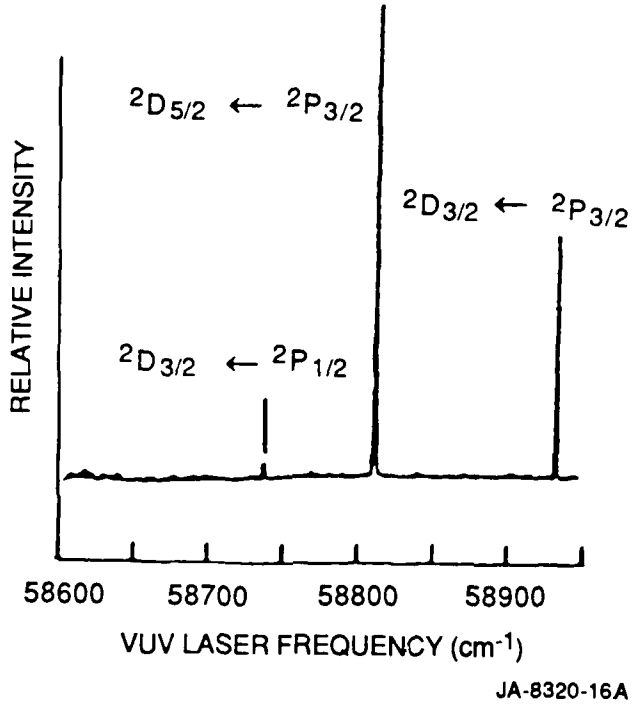

Figure 4. Two-photon-excited fluorescence excitation spectrum in atomic fluorine obtained using the sixth anti-Stokes radiation from a doubled dye laser.

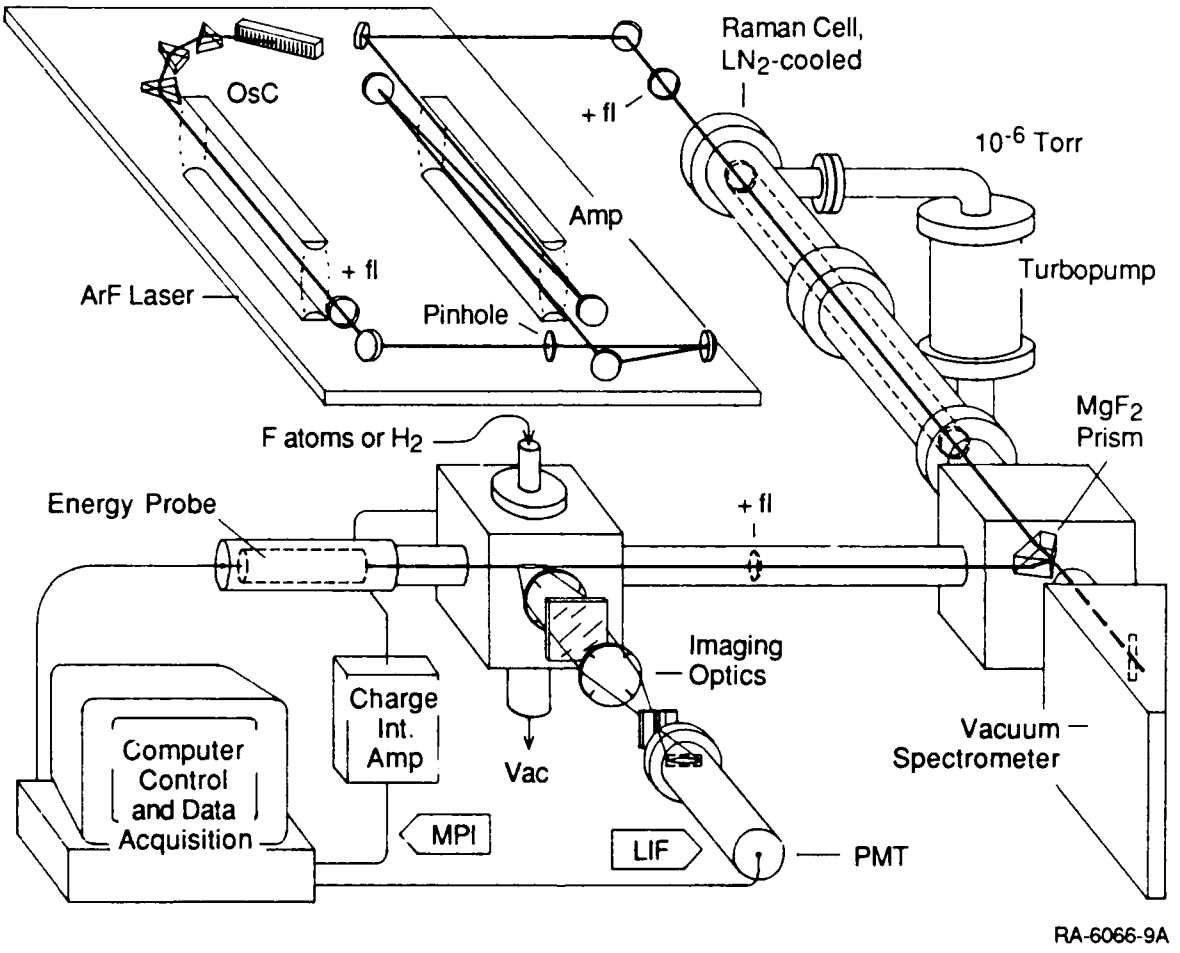

Figure 5. Apparatus for Raman shifting a tunable ArF laser for multiphoton excitation of F and F_2.

+ fl = positive focal length lens, MPI = multiphoton ionization, LIF = laser-induced fluorescence, PMT = photomultiplier.

doubled Nd:YAG-pumped dye laser was passed through the oscillator and amplifier discharges separately, and the windows were rotated to minimize the depolarization of the transmitted light. After this adjustment, the amplitude stability was quite good and the output was polarized to 200:1. With all of the modifications, the output energy is ~60 mJ, which is lower than the energy with the injection-locked amplifier (~100 mJ), but the better spatial mode quality allows significantly higher Raman shifting efficiency. The tuning range for the ArF laser using a double pass through the amplifier is shown in Figure 6. The dips in the curve are produced by the (4,0) and (7,1) Schumann-Runge bands of O_2. The depth of the bands has been enhanced by passing the ArF light through ~8 m of air.

The liquid nitrogen temperature Raman cell is shown in Figure 7. HD or D_2 is contained in the central gas cell, with a fused silica window on the input and a MgF_2 window on the output. Both windows are sealed with indium seals to allow operation at liquid nitrogen temperatures. The gas cell is surrounded along its length with a jacket for liquid nitrogen. The entire cell and liquid nitrogen jacket are enclosed in a vacuum jacket that serves three functions: (1) provision of insulation for the liquid nitrogen, (2) elimination of condensation on the end windows of the inner cell, and (3) provision of direct coupling to the evacuated downstream beam path for the generated vuv light. To minimize conduction between the liquid nitrogen jacket and the outer cell, the inner cell and jacket are supported only by the two tubes used for introduction of liquid nitrogen into the center of the cell.

We have examined the capabilities of this system for Stokes and anti-Stokes production for both HD and D_2. Although Raman scattering of a broadband ArF laser in D_2 has been demonstrated,[12] Raman shifting of ArF laser light in HD has not been investigated previously. A variety of effects affect the Raman conversion efficiency, and it is important to understand them. An example of the sensitivity of Raman conversion to the input beam is illustrated in Figures 8, 9, and 10. The first Stokes beam was monitored while the focusing lens was being used to vary the focus in the Raman cell, as shown in Figure 8. When the input lens is tilted, the Stokes beam exhibits the unexpected behavior shown in Figure 9. There is actually a minimum in the production of first Stokes radiation when the lens is normal to the laser beam, and the maxima occur with a slight tilt of the lens. Competition between the first Stokes and first anti-Stokes beams may explain this phenomenon.[13] The effect of moving the lens to change the spot size and Rayleigh range of the ArF beam in the cell is shown in Figure 10. Because the beam's Rayleigh range is within the cell for the range of lens translation in the figure, it appears that there is an optimum spot size and Rayleigh range for the first Stokes conversion. Conversion of more than 60% of the ArF laser power into the first Stokes order in D_2 has been obtained.

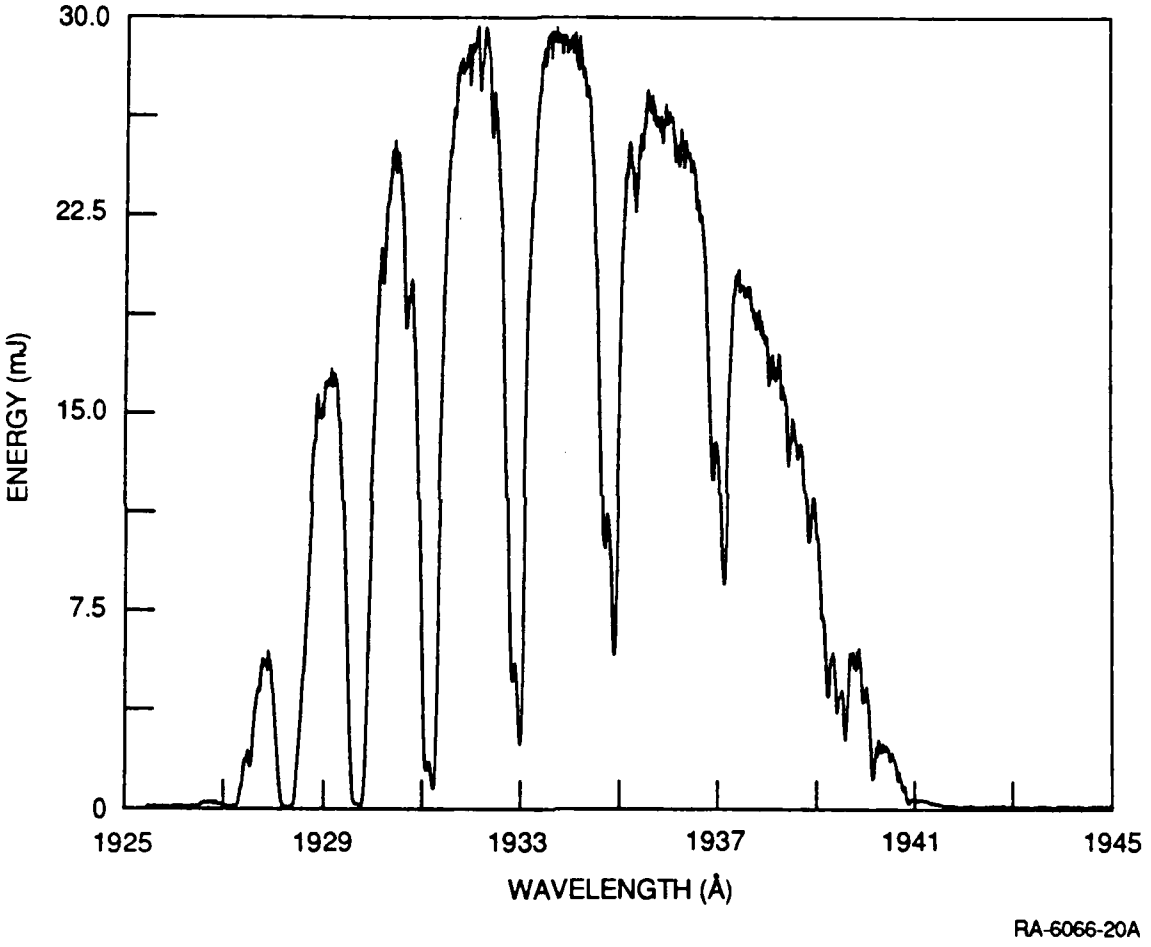

Figure 6. Tuning range of ArF laser with Schumann-Runge adsorption.

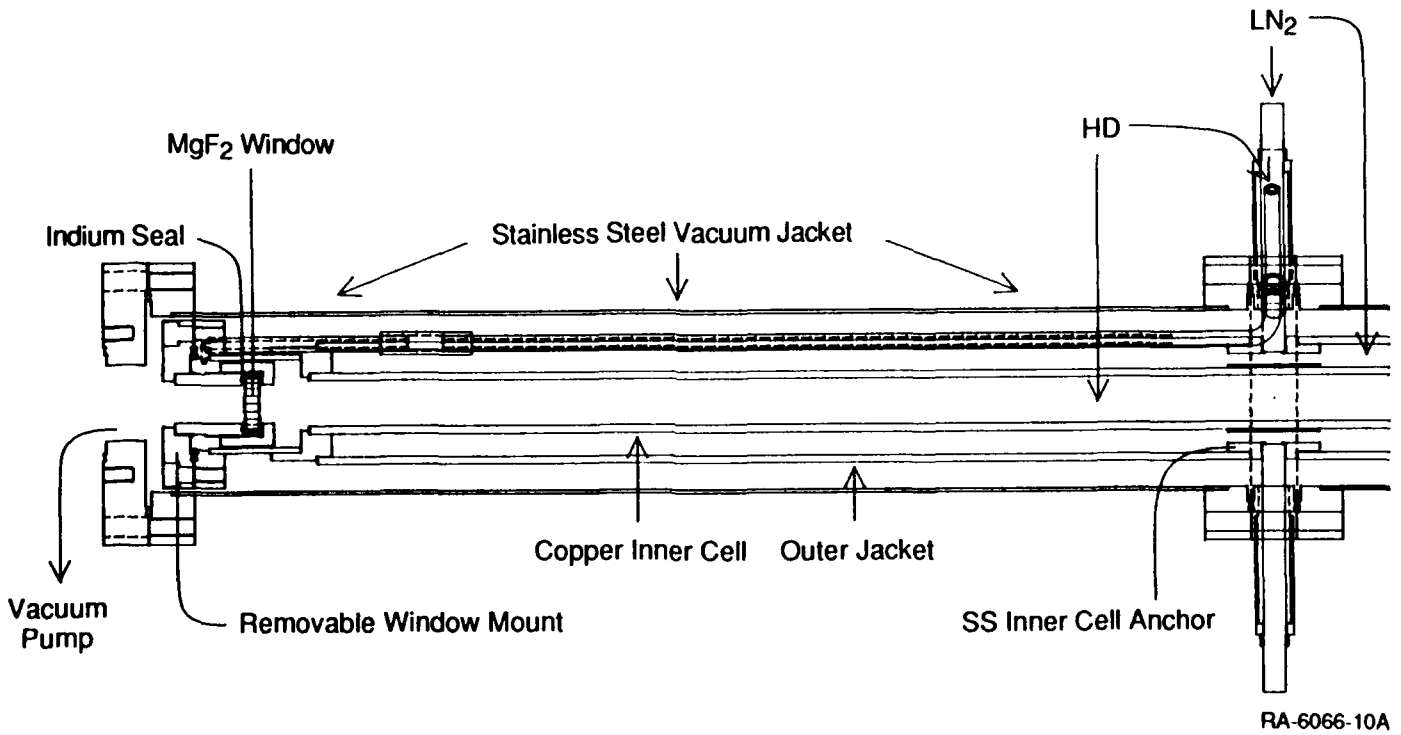

Figure 7. Liquid-nitrogen-cooled Raman cell.

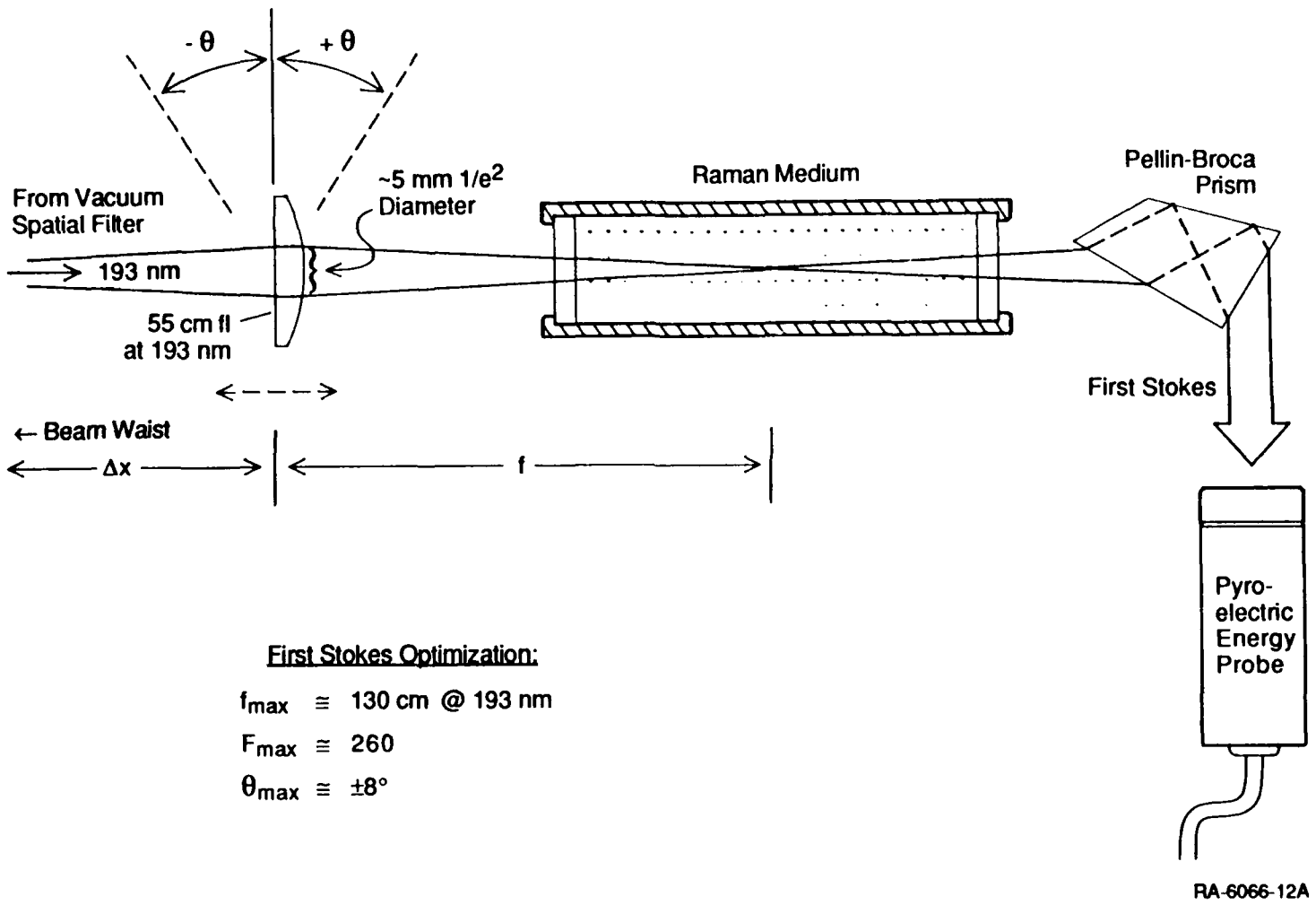

Figure 8. Diagram of first Stokes optimization in D_2.

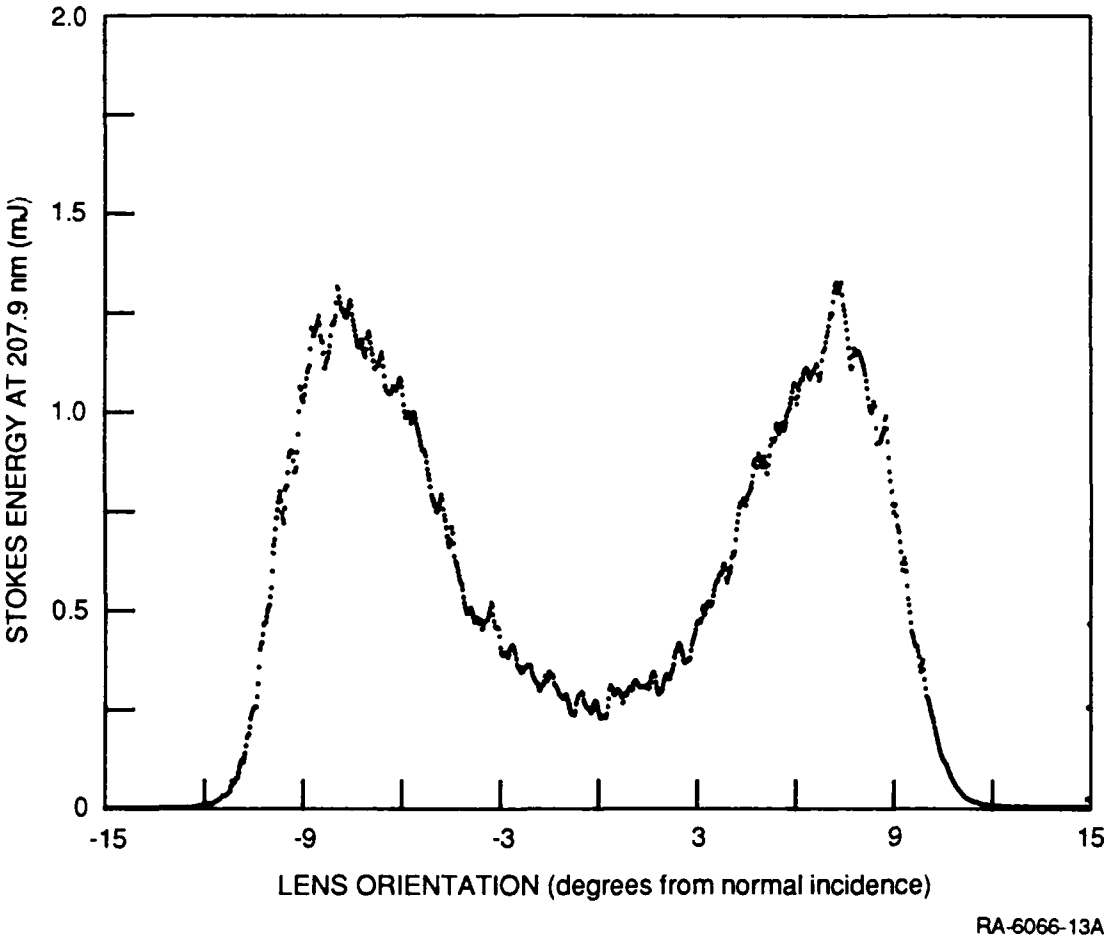

Figure 9. Dependence of first Stokes energy on tilt of focusing lens.

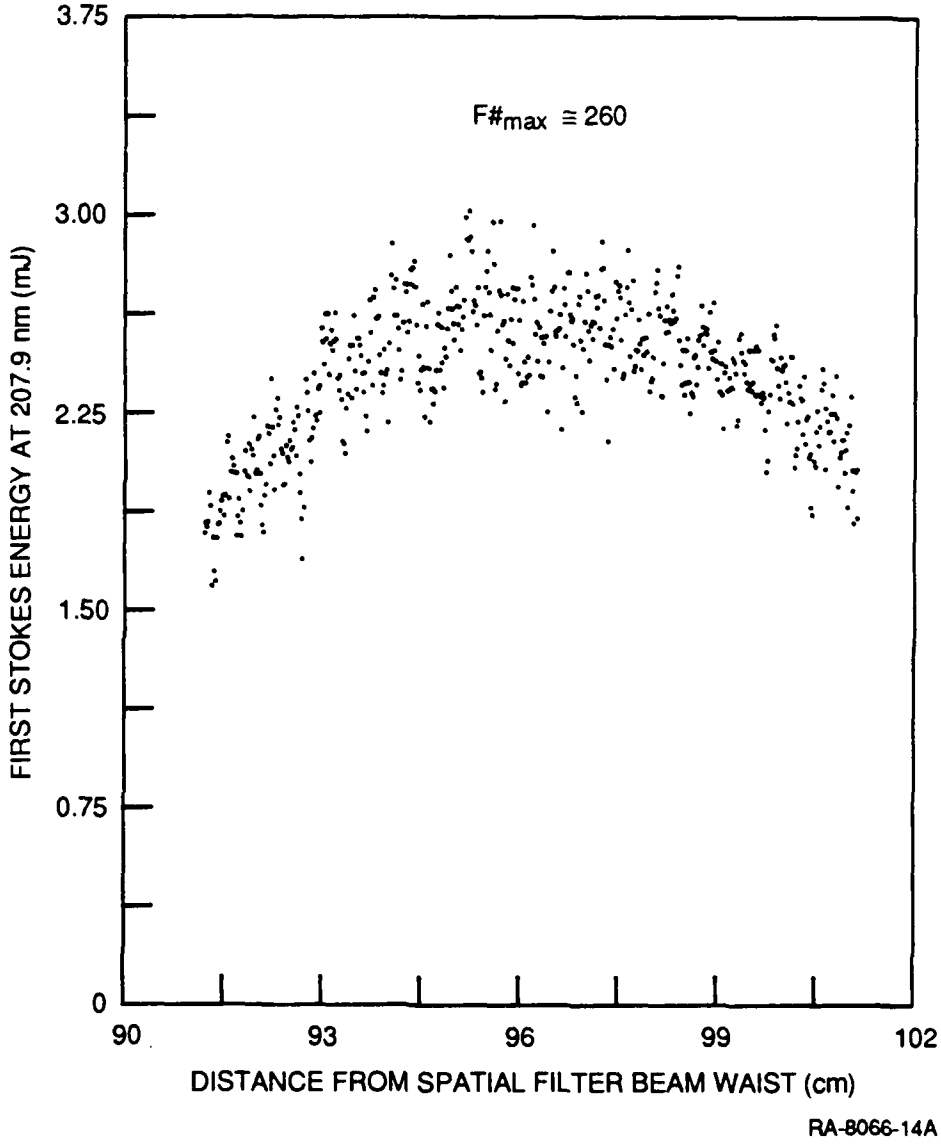

Figure 10. Dependence of first Stokes energy on lens position.

We used a vacuum spectrometer to observe the vibrational Stokes and anti-Stokes orders scattered from a scattering plate. At least eight anti-Stokes orders (to 132 nm) and five Stokes orders were observed for shifting in D_2. At least four anti-Stokes and four Stokes orders were observed for shifting in HD. Some of the anti-Stokes and Stokes orders generated are shown in Figures 11 and 12. Figure 11 shows lines generated in D_2 at room temperature and a density of 5.4 amagat. (One amagat is the density of an ideal gas at standard temperature and pressure.) Figure 12 shows Raman orders generated in HD at 77 K and a density of 6 amagat. The intensities shown have not been corrected for the wavelength response of the photomultiplier, spectrometer, and a filter used to reduce the intensity of the pump and Stokes orders.

A few rotational lines appear on the lines generated in HD. These become accentuated at lower densities. The explanation for this accentuation involves the nature of the gain dependence for stimulated Raman scattering on density. The stimulated Raman gain is proportional to the number of molecules and inversely proportional to the linewidth of the Raman transition. When the dominant contribution to the linewidth is from pressure broadening, the linewidth is proportional to the density, and the Raman gain is independent of density. As the density drops, the linewidth is ultimately limited by the Doppler linewidth, and the gain decreases with decreasing density. Because the Doppler width for the rotational Raman lines is much less than the vibrational Doppler width, the rotational Raman gain is independent of density to lower densities than for vibrational Raman scattering, and the rotational Raman scattering becomes larger relative to the vibrational Raman scattering. This is apparent in Figure 13, which shows the Raman orders in HD at a density of 3 amagat. The rotational lines are much larger than those shown for 6 amagat shown in Figure 12. While the loss of laser power into the rotational Raman orders can be reduced at higher densities, the phase matching process necessary for generation of higher order Raman lines is hampered at higher densities owing to the increase in the index of refraction and the increasing importance of dispersion. The combined effects of phase matching and rotational Raman generation are shown well in Figure 14 which shows Raman orders in D_2 at 77 K. For low densities, the vibrational Stokes and anti-Stokes orders are very small due to the dominance of rotational scattering. At higher densities, the higher order Stokes and anti-Stokes orders become larger, and at even higher densities, the higher order anti-Stokes lines become smaller again as a result of poorer phase matching.

The dependence of phase matching and Raman linewidth on density leads to an optimum density for generation of Raman lines. The density dependence of the energy in the second anti-Stokes vibrational line in HD is shown in Figure 15. This is the anti-Stokes order that can be used for detection of F atoms. The energy peaks at a density of about 3 amagat, where an energy of

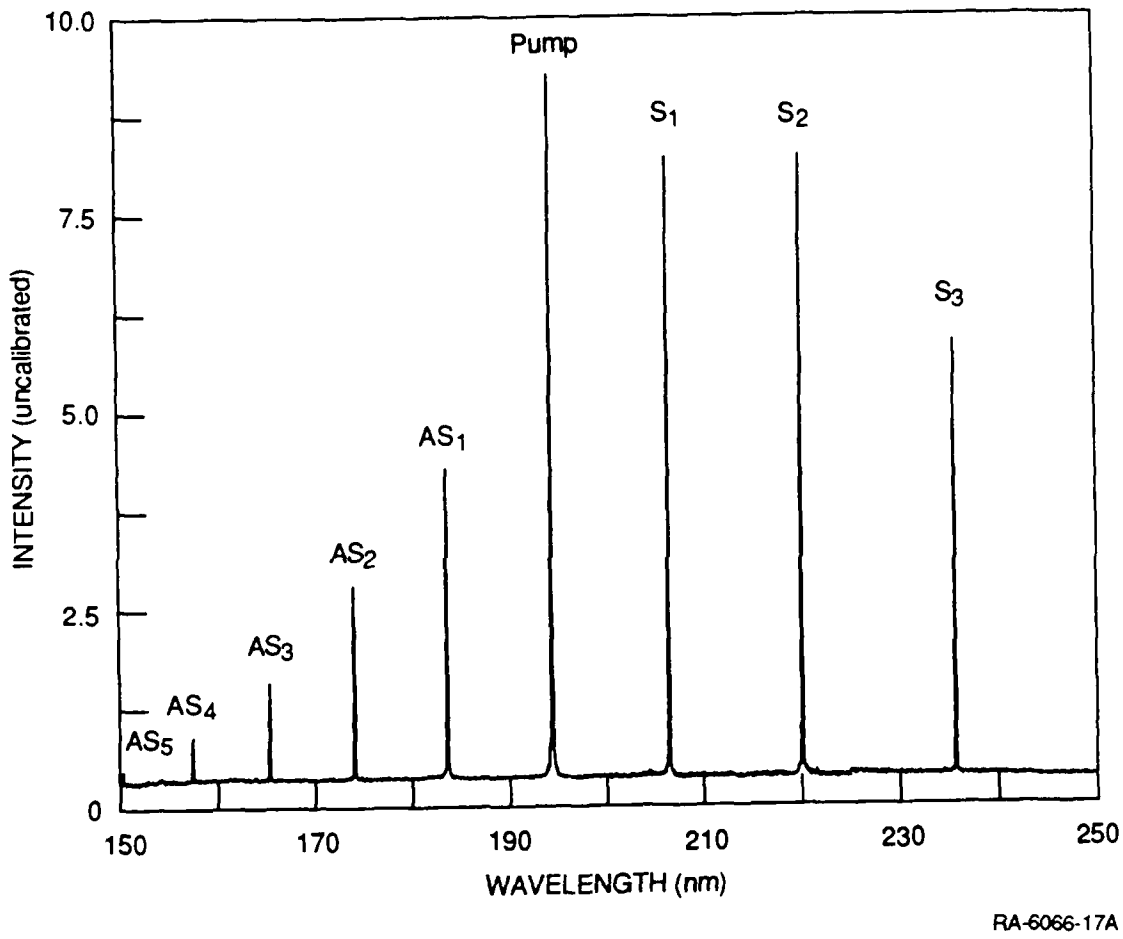

Figure 11. Stokes and anti-Stokes orders generated in D_2 at room temperature and a density of 5.4 amagat.

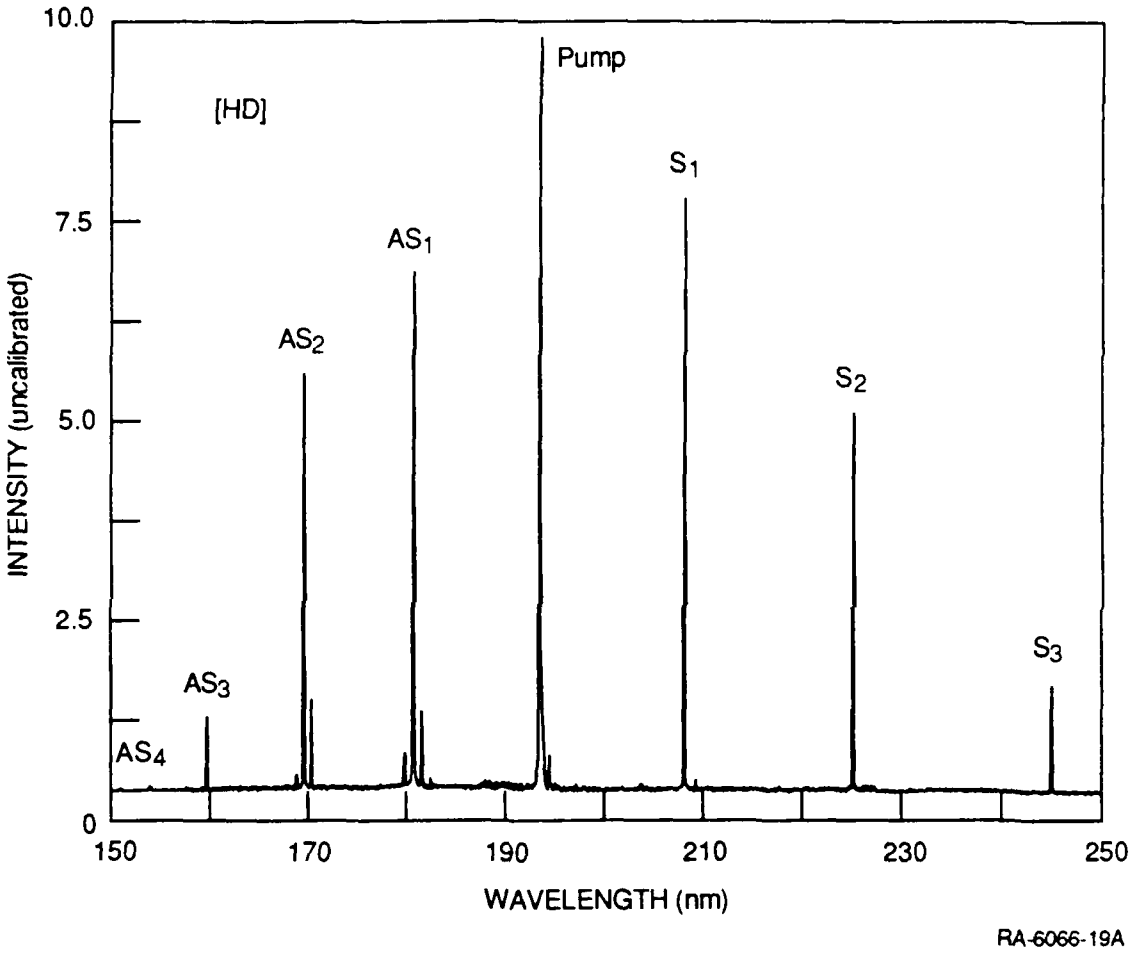

Figure 12. Stokes and anti-Stokes orders generated in HD at 77 K and a density of 6 amagat.

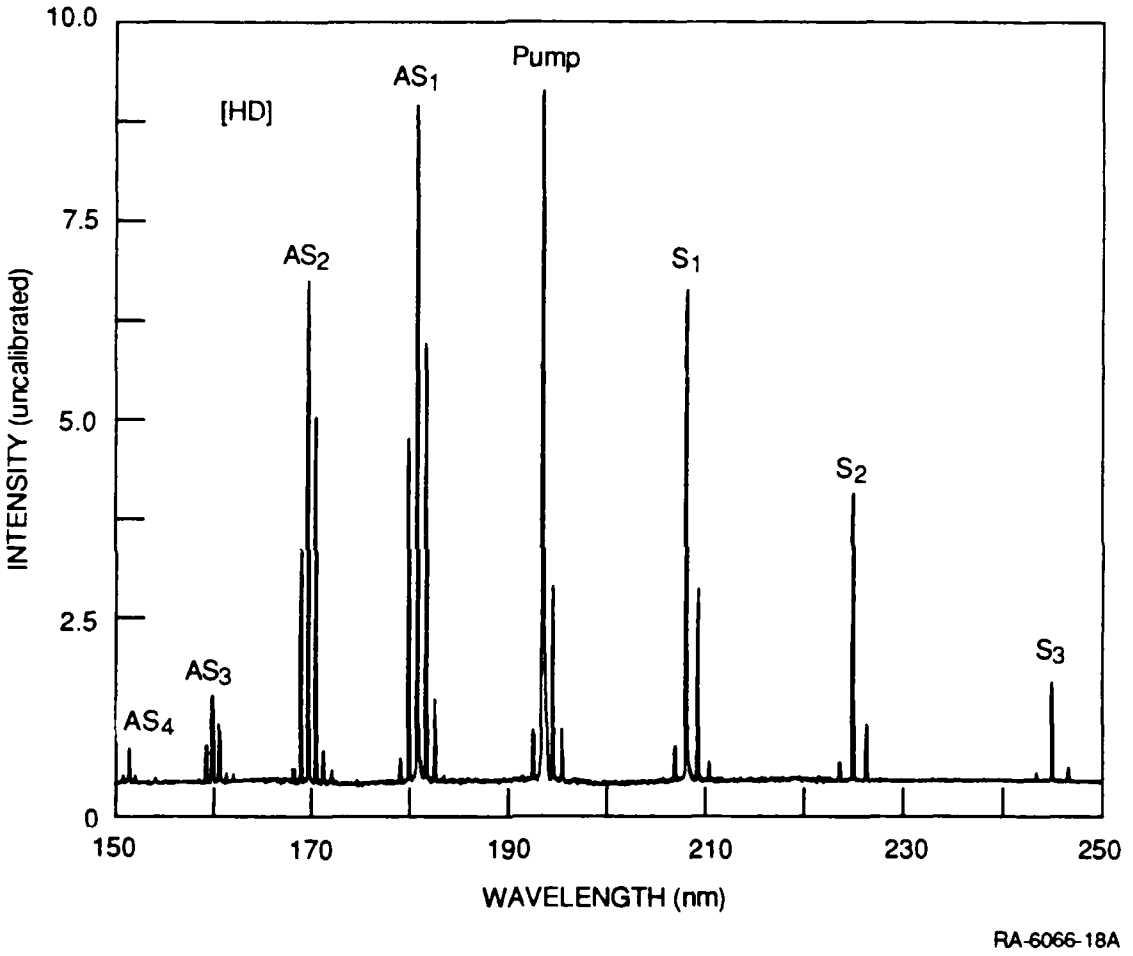

Figure 13. Stokes and anti-Stokes orders generated in HD at 77 K and a density of 3 amagat.

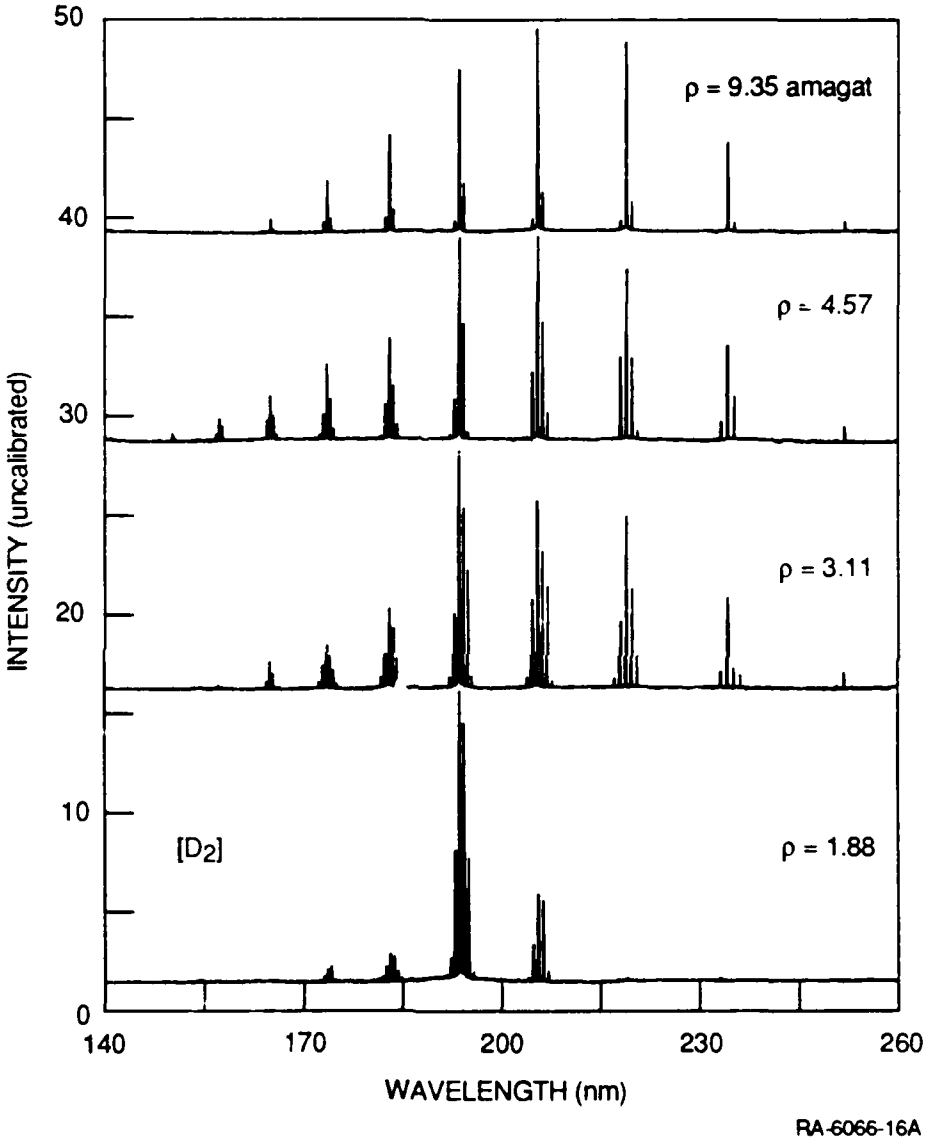

Figure 14. Raman orders in D_2 as a function of density at 77 K.

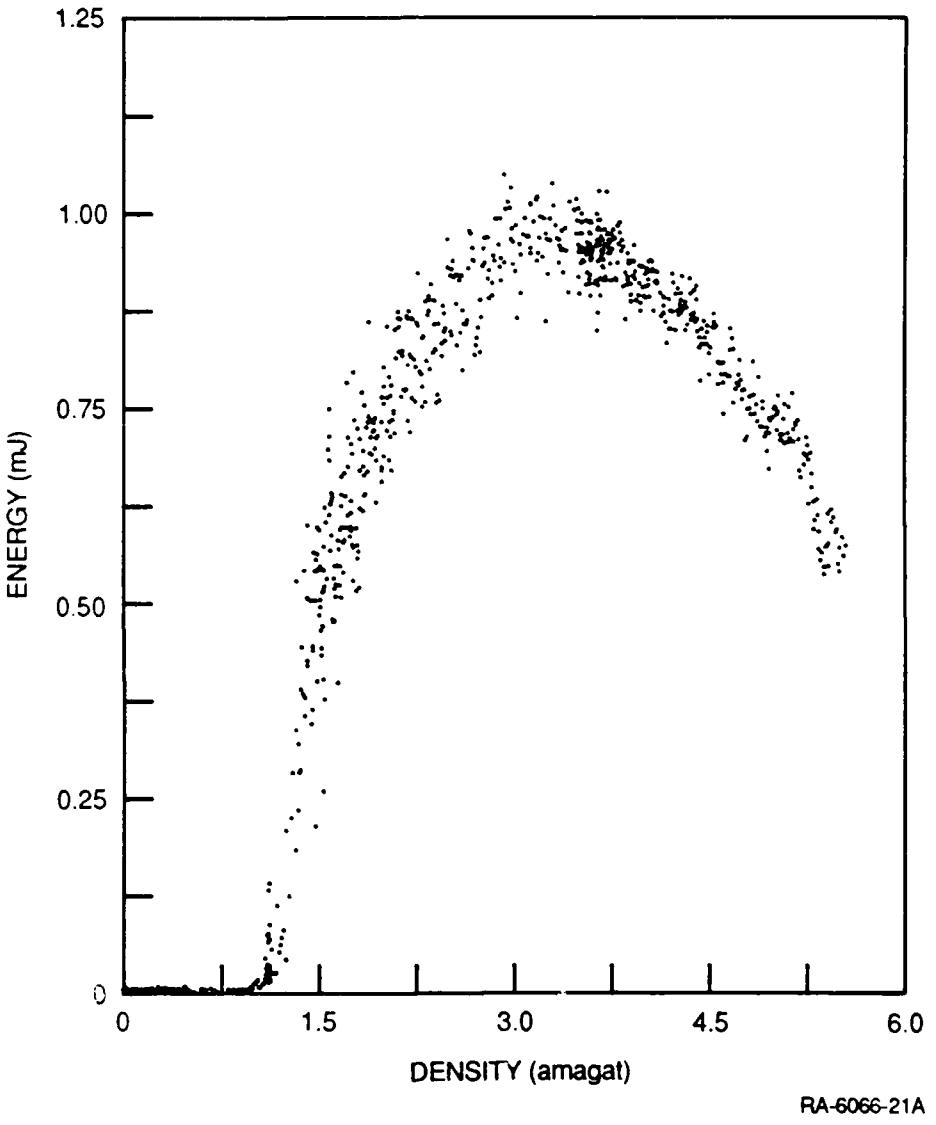

Figure 15. Density dependence of the second anti-Stokes radiation in HD.

about 1 mJ is produced. This is two orders of magnitude more energy than was produced previously by Raman shifting the frequency-doubled output of a Nd:YAG-pumped dye laser.

A prism was used to separate the Raman-shifted orders from the main ArF beam, as shown in Figure 5. Although a mirror could also be used, the prism is not wavelength specific. Thus, any of the Raman orders may be selected by rotation of the prism, which is performed with a motorized rotation stage. For transmission of the vuv wavelengths, a prism of MgF_2, CaF_2, or LiF must be used. Because both CaF_2 and LiF form color centers on irradiation with an intense uv or vuv beam such as the ArF laser, MgF_2 must be used. MgF_2, however, is birefringent, and if the input beam is not highly polarized, the depolarized portion of the beam is refracted at a different angle. This caused a particular problem with the second-order anti-Stokes line in HD, which is used for F atom detection. The difficulty is illustrated in Figure 16. The ordinary and extraordinary indices of refraction for MgF_2, n_o and n_e, are shown as a function of frequency in the vuv; n_o is the index for the laser polarization with low loss through the prism. Also shown are the frequencies for the second anti-Stokes orders in the isotopes of hydrogen. It is apparent that the refractive index for the main second-anti-Stokes beams, n_o, is the same as the refractive index for the depolarized ArF beam, n_e. This is unfortunate because the result is that depolarized ArF beam is refracted at the same angle as the second anti-Stokes beams and, because the ArF beam is so intense, a small amount of depolarization can lead to a beam stronger than the second anti-Stokes beam. This problem was solved through careful control of the polarization of the ArF laser, as described above, and the use of Brewster-angle fused silica plates in the ArF beam before the Raman cell to reject depolarized light.

The results of application of this vuv source to multiphoton excitation of various species are shown in Figure 17. Shown at the bottom of the figure are lines from the E,F($v' = 6,7$) state of H_2 that form two-photon resonances within the tuning range of the fundamental ArF beam. These are easy to excite and detect using an ion signal, and they allow calibration of the ArF wavelength. As an initial experiment, the H, $\bar{H}$ ($v' = 1$) state in H_2 was excited. This state is similar to the state in the F atom experiment in that it can also be detected with 2 + 1 resonantly-enhanced multiphoton ionization (REMPI) using second anti-Stokes radiation from the ArF laser. However, D_2 gas is used instead of HD, so the experiment can be done at room temperature. The signal lies very close to one of the E,F levels excited by the fundamental radiation, but it is clearly visible on the flank of the line, as seen in the lower right of the figure. All of the spectra in Figure 17 are plotted as a function of the fundamental ArF laser wavelength. By using HD at liquid nitrogen temperatures, a 2 + 1 REMPI signal of the $^2D^o_{3/2} \leftarrow {}^2P^o_{3/2}$ transition in atomic fluorine was obtained. This signal is shown in the upper right corner of Figure 17. Fortunately, the wavelength for production of radiation for F atom detection lies between the Schumann-Runge absorption bands shown in

Figure 6, so purging of the beam paths with nitrogen is not necessary. Detection of F_2 was also attempted using 2 + 1 REMPI with the first Stokes beam from Raman scattering in D_2. The result is shown in the upper left corner of Figure 17. The shape of the excitation spectrum is the same as that in Figure 1, except that the Schumann-Runge absorption obscures part of the the spectrum. The strongest peaks, however, lie between the Schumann-Runge bands.

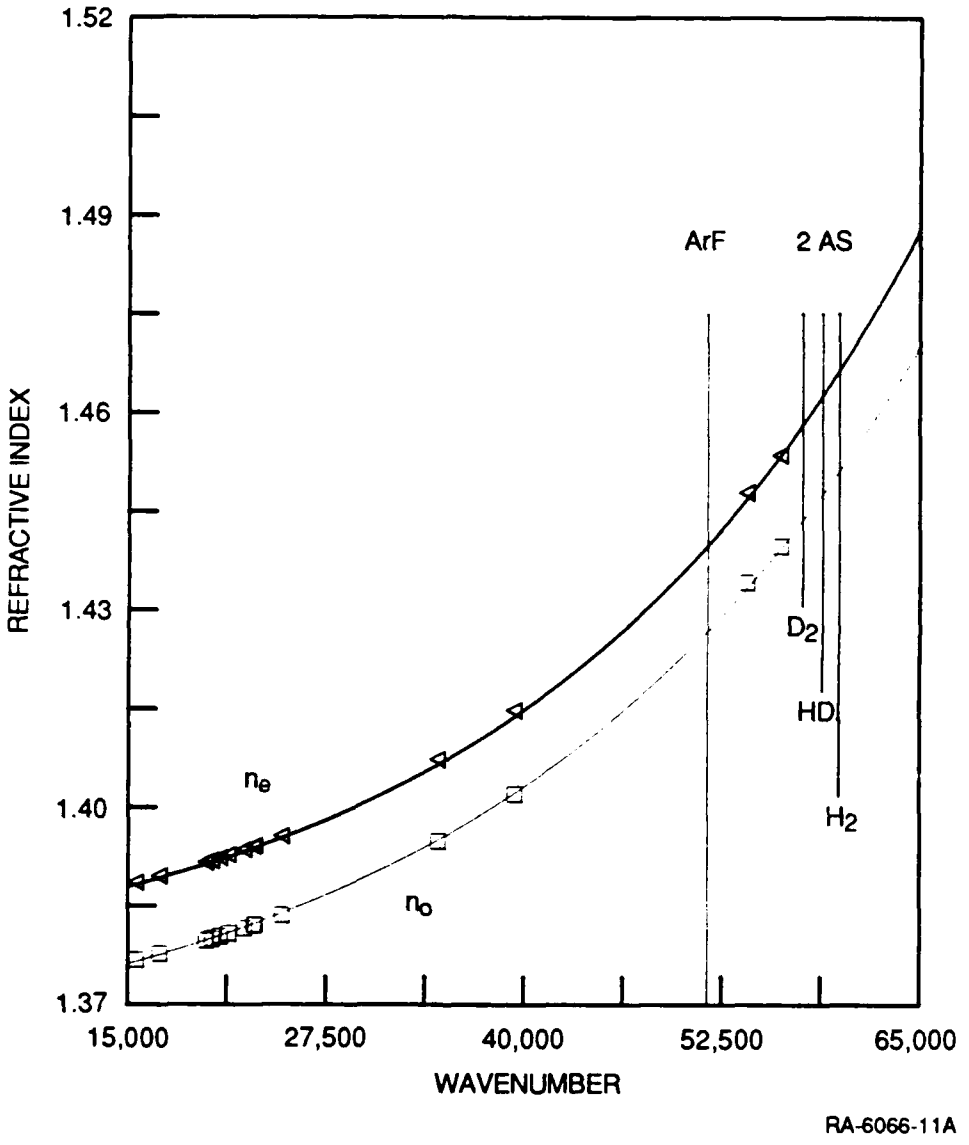

Figure 16. Refractive indices of MgF_2 for ArF and the second anti-Stokes (2 AS) frequencies.

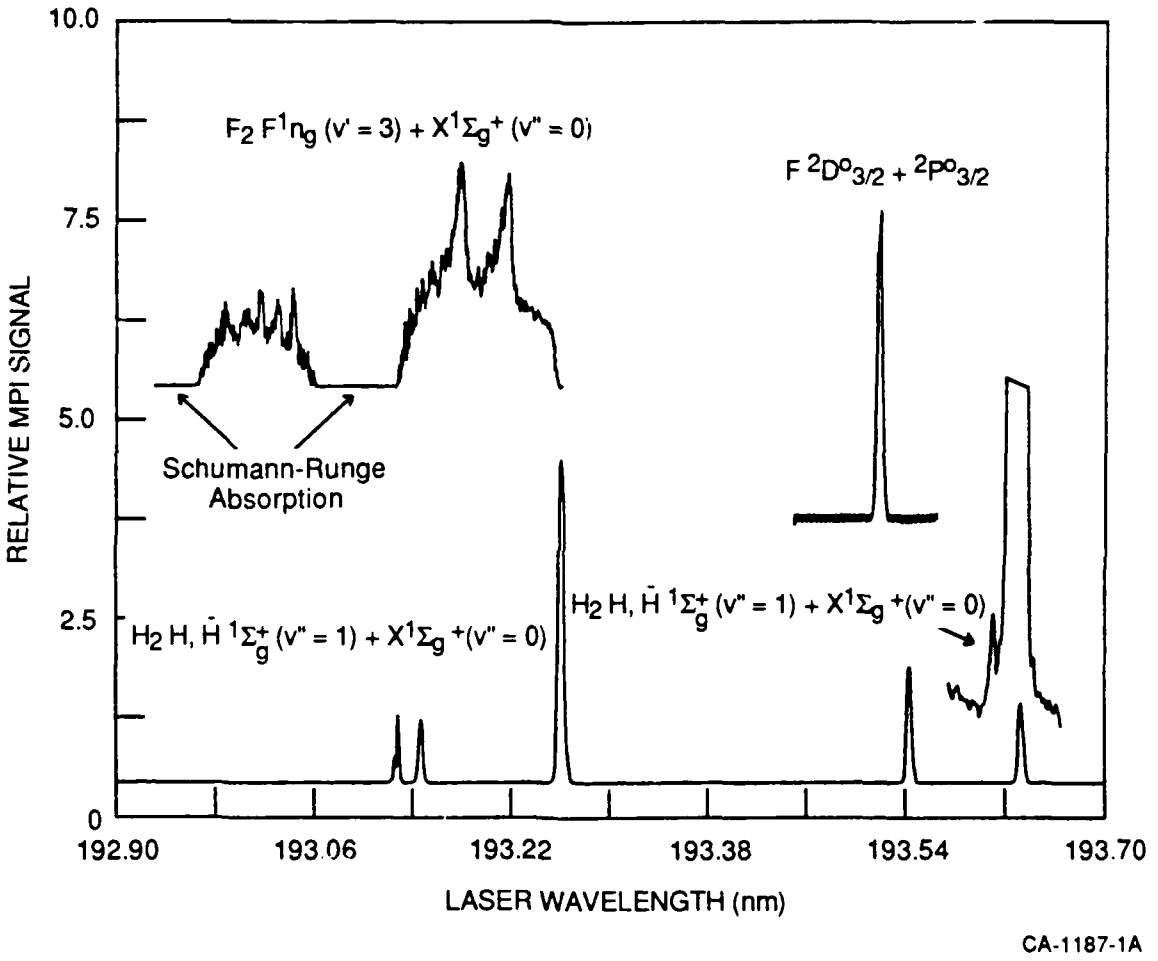

Figure 17. Spectra of lines in F atoms, F_2, and H_2 obtained with the fundamental and Raman orders of the ArF laser.

CONCLUSIONS

Substantial progress has been made in the multiphoton detection of F and F_2. A two-photon excitation scheme has been demonstrated for F_2 that uses both 2 + 1 REMPI and two-photon-resonant excited fluorescence. The excitation and emission spectra have been studied for better understanding of the detection mechanism. A high power uv-vuv laser source has been developed using Raman shifting of a tunable ArF excimer laser. This source has been applied to detection of both F and F_2.

REFERENCES

1. Michael A. A. Clune and Wing S. Nip, "Kinetic Spectroscopy in the Far Vacuum Ultraviolet," JCS Faraday Trans. II **73**, 1308-1319 (1977).

2. Howard Schlossberg, "Fluorine-Atom Probe Techniques for Chemical Lasers," J. Appl. Phys. **47**, 2044-2045 (1976).

3. Alan C. Stanton and Charles E. Kolb, "Direct Absorption Measurement of the Spin-Orbit Splitting and $^2P_{1/2}$ Radiative Lifetime in Atomic Fluorine ($2p^5$)," J. Chem. Phys. **72**, 6637-6641 (1980).

4. Glenn A. Laguna and Williard H. Beattie, "Direct Absorption Measurement of the Spin-Orbit Splitting of the Ground State in Atomic Fluorine," Chem. Phys. Lett. **88**, 439-440 (1982).

5. J. Wormhoudt, A. C. Stanton, and J. Silver, "Spectroscopy Characterization Techniques for Semiconductor Technology" Proc. SPIE **452** (1983).

6. C. Herring, M. J. Dyer, L. E. Jusinski, and W. K. Bischel, Opt. Lett. **13**, 360 (1988).

7. William K. Bischel and Leonard E. Jusinski, "Multiphoton Ionization Spectroscopy of Atomic Fluorine," Chem. Phys. Lett. **120**, 337-341 (1985).

8. Hideo Okabe, *Photochemistry of Small Molecules* (John Wiley and Sons, New York, 1978) p. 184.

9. Gregory W. Faris, Mark J. Dyer, William K. Bischel, and David L. Huestis, "Two-Photon Spectroscopy of the $F^1\Pi_g$ and $f^3\Pi_g$ States of Molecular Fluorine," to be submitted to Chem. Phys. Lett. (1990).

10. J. B. Halpern, H. Zacharias, and R. Wallenstein, J. Mol. Spectrosc. **79**, 1 (1980).

11. W. K. Bischel, "Two-Photon Techniques for Atomic Fluorine," Final Report of AFOSR Contract No. F49620-85-K-0005, SRI International, Menlo Park, California (June 1988).

12. T. R. Loree, R. C. Sze, D. L. Barker, and P. B. Scott, "New Lines in the UV: SRS of Excimer Laser Wavelengths," IEEE J. Quantum Electron. **QE-5**, 337-342 (1979).

13. A. P. Hickman and W. K. Bischel, "Stokes–Anti-Stokes Gain Suppression in the Transient Regime," Proc. SPIE **874**, 151-158 (1988).

PROFESSIONAL PERSONNEL

The following professional scientists participated in the research supported by this contract:

- **Gregory W. Faris, Physicist, SRI International**
  Lead experimentalist throughout the contract, and task leader since December 1988.

- **Mark J. Dyer, Physics Associate, SRI International**
  Specialist in lasers and nonlinear optics, made many of the major technical accomplishments. Part time student at San Jose State University.

- **William K. Bischel, Program Manager, SRI International**
  (At SRI until December 1988--presently at Coherent Inc., since December 1988)
  Project Leader and Principal Investigator until December 1988, continuing technical advisor since December 1988.

- **David L. Huestis, Associate Director, SRI International**
  Project Leader and Principal Investigator since December 1988, technical contributor, especially on theory and spectroscopy.

PATENT DISCLOSURES

The following patent disclosures are being prepared on inventions developed under this contract:

1. Two-Photon Detection Scheme for Molecular Fluorine
   Inventors: Gregory W. Faris, Mark J. Dyer, and William K. Bischel

2. High Mode Quality Tunable Excimer Laser
   Inventors: Mark J. Dyer, Gregory W. Faris, and William K. Bischel

3. Detection of Atomic Fluorine with Raman-Shifted ArF Radiation
   Inventors: Mark J. Dyer, Gregory W. Faris, and William K. Bischel

PUBLICATIONS ACKNOWLEDGING THIS CONTRACT

The following publications are being prepared on research supported by this contract:

1. Gregory W. Faris, Mark J. Dyer, William K. Bischel, and David L. Huestis, "Two-Photon Spectroscopy of the $F^1\Pi_g$ and $f^3\Pi_g$ States of Molecular Fluorine," in preparation for submission to Chemical Physics Letters.

2. Mark J. Dyer, William K. Bischel, and Gregory W. Faris, "Oscillator Triple-Pass Amplifier ArF Laser for Nonlinear Applications," in preparation for submission to Applied Optics.

3. Mark J. Dyer, William K. Bischel, and Gregory W. Faris, "Raman Shifting an ArF Laser in HD for Efficient Detection of Atomic Fluorine," in preparation for submission to the Journal of Chemical Physics.

TECHNICAL INTERACTIONS

The following conference talks and posters were presented on research supported by this contract. Each of these presentations generated number of questions and discussions.

1. "Multiphoton detection techniques for F and F_2," W. K. Bischel, talk presented at the 1988 AFOSR Contractors' Meeting, June, 14-16, 1988, Monrovia, CA.

2. "Two-photon spectroscopy of the $F^1\Pi_g$ and $f^3\Pi_g$ states of molecular fluorine," G. W. Faris and W. K. Bischel, talk presented at the Annual Meeting of the Optical Society of America, October 31 - November 4, 1988, Santa Clara, California.

3. "Detailed Study of the Upper Level of the Fluorine Laser at 157.5 nm," G. W. Faris, M. J. Dyer, and W. K. Bischel, poster presented at the Conference on Quantum Electronics and Laser Science, April 24-28, 1989, Baltimore, Maryland.

4. "Two-Photon Spectroscopy of the $F^1\Pi_g$ and $f^3\Pi_g$ States of F_2" G. W. Faris, M. J. Dyer, W. K. Bischel, and D. L. Huestis, talk presented at the Forty-Fourth Symposium on Molecular Spectroscopy, June 12-16, 1989, Ohio State University, Ohio.

5. "Two-Photon Detection of and F_2," Paper A-2, G. W. Faris, M. J. Dyer, W. K. Bischel, and D. L. Huestis, talk presented at the Forty Second Annual Gaseous Electronics Conference, September 17-20, 1989, Palo Alto, California.

6. "Multiphoton Spectroscopy of and F_2," G. W. Faris, M. J. Dyer, W. K. Bischel, and D. L. Huestis, invited talk presented at the International Conference on LASERS'89, December 3-8, 1989, New Orleans, Louisiana.

7. "VUV Stimulated Raman Scattering of an ArF Laser in D_2 and HD," G. W. Faris, M. J. Dyer, W. K. Bischel, and D. L. Huestis, poster presented at the Conference on Lasers and Electro-Optics, May 21-25, 1990, Anaheim, California.

8. "Novel Nonlinear Laser Diagnostic Techniques," David L. Huestis, Gregory W. Faris, and Jay B. Jeffries, talk presented at the 1990 AFOSR Contractors Meeting in Propulsion, June 11-15, 1990, Atlanta, Georgia.

We have served as informal advisors on aspects of the work supported by this contract in the following technical interactions:

Dr. Richard Miles and Dr. Walter Lempert, Princeton University, Princeton, New Jersey.

Subject: Raman shifting excimer lasers, liquid nitrogen temperature Raman cells, improvement of excimer laser beam quality.

Form of Communication: Conversations at the Conferences on Lasers and Electro-Optics, April 24-28, 1989, Baltimore, Maryland, and May 21-25, 1990, Anaheim, California, telephone conversations, 1989 and 1990.

Dr. Simon Hooker and Dr. C. E. Webb, Clarendon Laboratory, Oxford, Great Britain.

Subject: Mechanism of the F_2 laser.

Form of Communication: Conversations at the Conference on Lasers and Electro-Optics, April 24-28, 1989, Baltimore, Maryland, written correspondence, February-March 1990.

Dr. Bish Ganguli, Wright Research and Development Center

Subject: Wide ranging, development of diagnostic techniques.

Form of Communication: Conversations at the AFOSR/ONR Contractors Meetings on Propulsion (June 19-23, 1989, Ann Arbor, MI and June 11-15, 1990 Atlanta, GA) and at the Gaseous Electronics Conference (October 17-20, 1989, Palo Alto, CA and October 16-19, 1990, Chamgaign, IL).

Dr. H. F. Calcote, Aerochem, Princeton

Subject: Various, soot formation.

Form of Communication: Conversations at the AFOSR/ONR Contractors Meetings on Propulsion (June 19-23, 1989, Ann Arbor, MI and June 11-15, 1990 Atlanta, GA).

Dr. Robert McKenzie, NASA Ames Research Center, Moffett Field, CA

Subject: Diagnostic techniques.

Form of Communication: Visit to SRI, November 1989.

Dr. Robert Donovan, University of Edinburgh, Edinburgh, Scotland

Subject: F_2 spectroscopy.

Form of Communication: Visit to SRI, March 1990.

Dr. Phil Paul, Stanford University, Stanford, CA

Subject: ArF laser modification.

Form of Communication: Visit to SRI, spring, 1990.

Dr. Sune Svanberg and Dr. Stefan Kröll, Lund Institute of Technology, Lund, Sweden

Subject: Raman shifting dye lasers for vuv production, Raman shifting an ArF laser for excitation of doubly-ionized sulfur.

Form of Communication: Conversations, Conference on Lasers and Electro-Optics, May 21-25, 1990, written correspondence, October, 1990.

Dr. Arthur Fontijn, Rensselaer Polytechnic Institute, Troy, NY

Subject: Raman shifting an ArF excimer laser for detection of BF.

Form of Communication: Conversations at the AFOSR/ONR Contractors Meeting on Propulsion June 11-15, 1990 Atlanta, Georgia, telephone conversations, written correspondence, June-August 1990.

Prof. Karl Welge, University of Bielefeld, Germany

Subject: VUV generation from ArF lasers.

Form of Communication: Visit to SRI, August 1990.

Dr. R. N. Compton, Oak Ridge National Laboratory

Subject: Dectection of F_2, especially by laser productions of F_2^+ .

Form of Communication: Telephone conversation, September 1990.

Dr. Michael Smith, Arnold Air Force Base, Tennessee.

Subject: Polarization optimization for excimer lasers.

Form of Communication: Telephone conversation, October 4, 1990.

APPENDIX

TWO-PHOTON SPECTROSCOPY OF THE $F^1\Pi_g$ AND $F^3\Pi_g$ STATES OF MOLECULAR FLUORINE

TWO-PHOTON SPECTROSCOPY OF THE $F^1\Pi_g$ AND $f^3\Pi_g$ STATES OF MOLECULAR FLUORINE

Gregory W. Faris, Mark J. Dyer, William K. Bischel, and David L. Huestis
Molecular Physics Laboratory
333 Ravenswood Avenue
Menlo Park, CA 94025

ABSTRACT

We report what is to our knowledge the first two-photon excitation spectroscopy of molecular fluorine. The $F^1\Pi_g$ and $f^3\Pi_g$ states are excited with two photons near 207 nm. Detection is through vuv fluorescence or ionization. Measurement of the fluorescence spectrum with a vuv spectrometer indicates that the vuv fluorescence occurs on the 157-nm F_2 laser transition.

To be submitted to: Chemical Physics Letters.

MP 90-140
August 1990

INTRODUCTION

The spectroscopy of molecular fluorine is not well known, partly because of the high ionization potential of this molecule. The lowest known bound state that can be reached in a spin-allowed transition from the ground state is the $F^1\Pi_g$ state, at about 93,000 cm^{-1} above the $X^1\Sigma_g^+$ ground state. Thus, much of the spectroscopy on the bound excited states of F_2 has been performed using vuv absorption spectroscopy.[1] The $F^1\Pi_g$ state is not accessible in an electric dipole-allowed transition from the ground state. This state and the nearby $f^3\Pi_g$ state have been observed in emission from the $I^1\Sigma_u^+$ state,[2] as well as by electron impact spectroscopy.[3-5] The $F^1\Pi_g$ state can be reached in a two-photon excitation from the ground state. Multiphoton excitation allows laser spectroscopy of the high-lying states in F_2, as was reported for the 3+1 resonantly-enhanced multiphoton ionization (REMPI) excitation of the H $^1\Sigma_u$ and h $^3\Sigma_{1u}^+$ states.[6]

In our studies of F_2, the vibrational levels v' = 0, 1, 2 of the $F^1\Pi_g$ state and v' = 3 of the $f^3\Pi_g$ state are excited from the ground $X^1\Sigma_g^+$ state by two photons and detected by vuv fluorescence or through ionization by a third photon. In addition to providing a means of detecting the ground state of F_2, the two-photon excitation scheme we describe may be useful in investigating the kinetics of the 157-nm F_2 laser.

Some calculated potential energy curves for F_2 are given in Figure 1. The lower states are taken from a publication by Cartwright and Hay,[7] while the upper two states are taken from the data of Sakai et al.[8] The upper states have been lowered from the position given by Sakai et al.to give the proper energy spacing for the $^1\Pi_g \leftarrow {}^1\Sigma_g^+$ and $^3\Pi_g \leftarrow {}^1\Sigma_g^+$ transitions. The 157-nm F_2 laser transition is believed to arise from a transition from the outer well of the $f^3\Pi_g$ state to a weakly bound $^3\Pi_u$ state. Even when the $f^3\Pi_g$ state is shifted down to give the proper energy spacing relative to the inner well, the outer well is still too high compared to the 157-nm transition to the lower state.

EXPERIMENT

The experimental arrangement for two-photon excitation of F_2 is shown in Figure 2. An excimer-pumped dye laser (Lambda Physik EMG102 and FL3002) with PBBO* dye produces about 6 mJ at 414 nm. This light is frequency doubled in a β-BaB_2O_4 crystal to give about 200 mJ at 207 nm. This light is focused with a 5-cm lens into a stainless steel cell containing a mixture of fluorine and helium. The fluorine-helium mixture is flowed slowly through the cell to maintain passivation. Ions are detected with a single electrode biased at 100 V relative to the cell. The ion signals are amplified with an Ortec model 142 PC charge-integrating preamplifier. Fluorescence is collected with a 5-cm MgF_2 lens and focused with a 25-cm MgF_2 lens onto the slits of a vacuum monochromator.

The fluorescence is detected with a CsI solar blind photomultiplier. The positions of the lenses are set to image the focal volume of the laser onto the slits and thus enhance the contrast between the fluorescence and the scattered laser light in the cell. For most of the fluorescence measurements, the vacuum monochromator is not used. One set of slits (removed from the vacuum monochromator) is placed at the image of the second lens, and the photomultiplier is placed directly behind the slits. In all cases, it is necessary to evacuate the entire fluorescence optical path to detect the fluorescence.

The 207-nm light that passes through the cell passes either through a calibration cell containing NO or onto a pyroelectric energy meter. The 1 + 1 REMPI signal from the $B^2\Pi \leftarrow X^2\Pi$ (3,0) band in NO is used as a wavelength calibration. The NO band is in turn calibrated against iodine fluorescence by operating the dye laser with an etalon at about 621 nm, doubling the frequency in a KDP crystal, and mixing the doubled and fundamental beams in the same β-BaB_2O_4 crystal used for direct doubling. Part of the remaining fundamental beam is directed to an iodine cell, while the mixed beam passes through the NO cell. Direct calibration of the F_2 signal

to iodine was not possible because the energy at 207 nm is not sufficient for F_2 excitation when the etalon is used, and the iodine spectra are not resolved without the etalon. The direct calibration could have been performed using a doubled Nd:YAG laser as a pump laser instead of the excimer laser with resultant higher resolution in the F_2 spectra, but such a pump laser was not available.

Ionization and fluorescence excitation spectra of the $F^1\Pi_g$ (v' = 2) state are shown in Figure 3. We have also observed the lower vibrational levels v' = 0 and 1, but with poorer signal-to-noise ratios. We have assigned the observed transitions on the basis of previous fluorescence[1] and electron-impact excitation experiments.[4] Five rotational bands ($\Delta J = 0, \pm 1, \pm 2$) are expected for this two-photon transition. The O and P branches form heads, while the other three branches are degraded to the blue, indicating that the rotational constant of the upper state is greater than that of the ground state. Also shown in Figure 3 is a spectral simulation. The line intensities are calculated from the two-photon Hönl-London factors given by Halpern et al.,[9] while the rotational energies for the $X^1\Sigma_g^+$ ground state are calculated from the constants given by Huber and Herzberg.[10] A room temperature Boltzmann population is assumed, and the linewidth, vibrational energy, and rotation constants for the upper $F^1\Pi_g$ state are used as fitting parameters. The agreement in structure between the theoretical and fluorescence spectra is good.

In Figure 4 are shown ionization and fluorescence excitation spectra for the transition $f^3\Pi_g$ (v' = 3) $\leftarrow$ $X^1\Sigma_g^+$ (v" = 0). The vibrational assignment is that of Hoshiba et al.[4] These spectra constitute the first two-photon singlet to triplet transition to our knowledge. A theoretical spectrum calculated in the same manner as for that in Figure 3 is also shown in Figure 4. The calculation does not take into account spin-orbit fine structure of the $f^3\Pi_g$ state. The agreement between the experimental and simulated spectra is not as good as for the singlet state, but the qualitative agreement suggests that the main source of transition probability is spin-orbit mixing of the $f^3\Pi_g$ (Ω=1) spin component with the $F^1\Pi_g$ (Ω = 1) state.

The emission spectrum observed through the vacuum spectrometer, when we excite v' = 2 of the $F^1\Pi_g$ state is shown in Figure 5. The emission spectrum from the $f^3\Pi_g$ state is very similar

to the one in Figure 5. These spectra agree very well with those observed in electron-excited F_2–rare gas mixtures.[11,12] The fluorescence for the $F^1\Pi_g$ state follows a third power of the laser power, indicating that population of the upper level of the fluorescence is probably occurring through ionization of F_2. This conclusion is supported by the increase in the fluorescence signal as the He pressure is increased, and by the time dependence of the fluorescence signal, which is shown in Figure 6 for various total pressures. Similar fluorescence time histories are obtained for excitation of either the $F^1\Pi_g$ or the $f^3\Pi_g$ state. The peak fluorescence signal is always delayed with respect to the laser pulse, the delay increasing as the total pressure in the cell decreases. This delay might be interpreted as being due to slowing of the possible excitation processes

$$F_2 + 3\,h\nu \rightarrow F_{2g}^{+} + e$$

$$e + F_2 \rightarrow F^- + F$$

$$F^- + F_2^{+} \rightarrow F_2^{*} + F$$

or

$$F_2 + 3\,h\nu \rightarrow F^* + F$$

$$F^* + F_2 \rightarrow F_2^{*} + F$$

This opens the possibility of study of the F_2 laser transition and kinetics using laser excitation.

An additional interesting result was found when the ionization signal was measured as a function of pressure. A set of such measurements is shown in Figure 7. The relative intensities of the different rotational lines change with pressure in a way that is not currently understood. This behavior was not present in the fluorescence spectra.

Many interesting and important measurements can be performed using the two-phootn excited fluorescnece (TPEF) detection technique that we have developed for F_2. The first of these is further experiments and analysis to understand the pressure dependence of the different rotational branches in three-photon ionization. Such a dependence further complicates the inference of species concentrations from ionization signals. Next in importance is a general

investigation of the collisional kinetics of the excited states of F_2. Only limited information is presently available,[13] partly because of the lack of a convenient excitation scheme, a problem we have just solved. Such studies should provide valuable information about various kinetic processes in the F_2 laser at 157 nm, the brightest source spectrally in the vuv today.

REFERENCES

1. E. A. Colbourn, M. Dagenais, A. E. Douglas, and J. W. Raymonda, "The Electronic Spectrum of F_2," Can. J. Phys. **540**, 1343-1359 (1976).

2. T. L. Porter, "Emission Spectrum of Molecular Fluorine," J. Chem. Phys. **48**, 2071-2083 (1968).

3. R.-G. Wang, Z.-W. Wang, M. A. Dillon, and D. Spence, "Electron Energy Loss Spectroscopy of Molecular Fluorine," J. Chem. Phys. **80**, 3574-3579 (1984).

4. K. Hoshiba, Y. Fujita, S. S. Kano, H. Takuma, T. Takayanagi, K. Wakiya, and H. Suzuki, "Experimental Observation of the F_2 VUV Laser Levels," J. Phys. B: At. Mol. Phys. **18**, L875-L879 (1985).

5. D. Spence, H. Tanaka, M. A. Dillon, and K. Lanik, "Direct Observation of 157 nm Laser Photons from the $f^3\Pi_g$ State of F_2 by High-Resolution Electron Impact," J. Phys. B: At. Mol. Phys. **19**, L569-L573 (1986).

6. W. K. Bischel and L. E. Jusinski, "Multiphoton Ionization Spectroscopy of Atomic Fluorine," Chem. Phys. Lett. **120**, 337-341 (1985).

7. D. C. Cartwright and P. J. Hay, J. Chem. Phys. **70**, 3191 (1979).

8. T. Sakai, K. Tanaka, A. Murakami, H. Iwaki, H. Terashima, and T. Shoda, J. Phys. B: At. Mol. Phys. **21**, 229 (1988).

9. J. B. Halpern, H. Zacharias, and R. Wallenstein, J. Mol. Spectrosc. **79**, 1 (1980).

10. K. P. Huber and G. Herzberg, *Molecular Spectra and Molecular Structure IV. Constants of*

Diatomic Molecules (Van Nostrand Reinhold Company, New York, 1979).

11. J. K. Rice, A. K. Hays, and J. R. Woodworth, Appl. Phys. Lett. **31**, 31 (1977).

12. M. Diegelmann, "Untersuchungen an molekularen Halogenlasern: Fluoreszenzspectroskopie, Reaktionskinetik und Laserexperimente," Dissertation, Ludwig-Maximillians-Universität, München (1980).

13. D. L. Huestis, R. M. Hill, H. H. Nakano, and D. C. Lorents, J. Chem. Phys. **69**, 5133 (1978).

FIGURE CAPTIONS

1. Calculated potential curves of some states in F_2.

2. Experimental schematic for F_2 detection.

3. F_2 $F^1\Pi_g$ ($v' = 2$) $\leftarrow$ $X^1\Sigma_g^+$ ($v'' = 0$) two-photon spectra.

4. F_2 $f^3\Pi_g$ ($v' = 3$) $\leftarrow$ $X^1\Sigma_g^+$ ($v'' = 0$) two-photon spectra.

5. VUV emission on excitation of the F_2 $F^1\Pi_g$ ($v' = 2$) state.

6. Pressure dependence of the F_2 $F^1\Pi_g$ ($v' = 2$) state fluorescence signal.

7. F_2 $F^1\Pi_g$ ($v' = 2$) $\leftarrow$ $X^1\Sigma_g^+$ ($v'' = 0$) MPI spectra as a function of pressure.

---

* PBBO = 2-(4-biphenyl)-6-phenylbenzoxatol-1,3

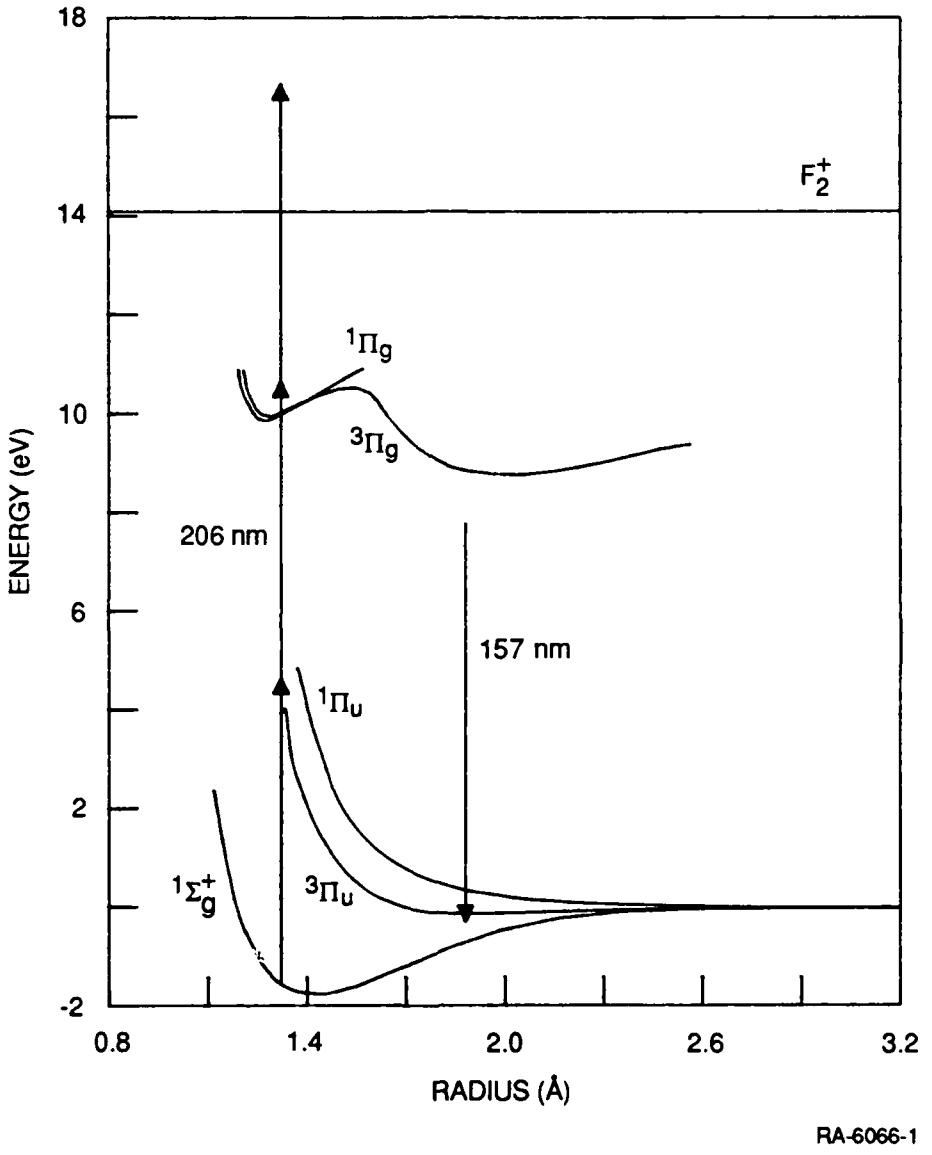

Figure 1. Calculated potential curves of some states in F_2.

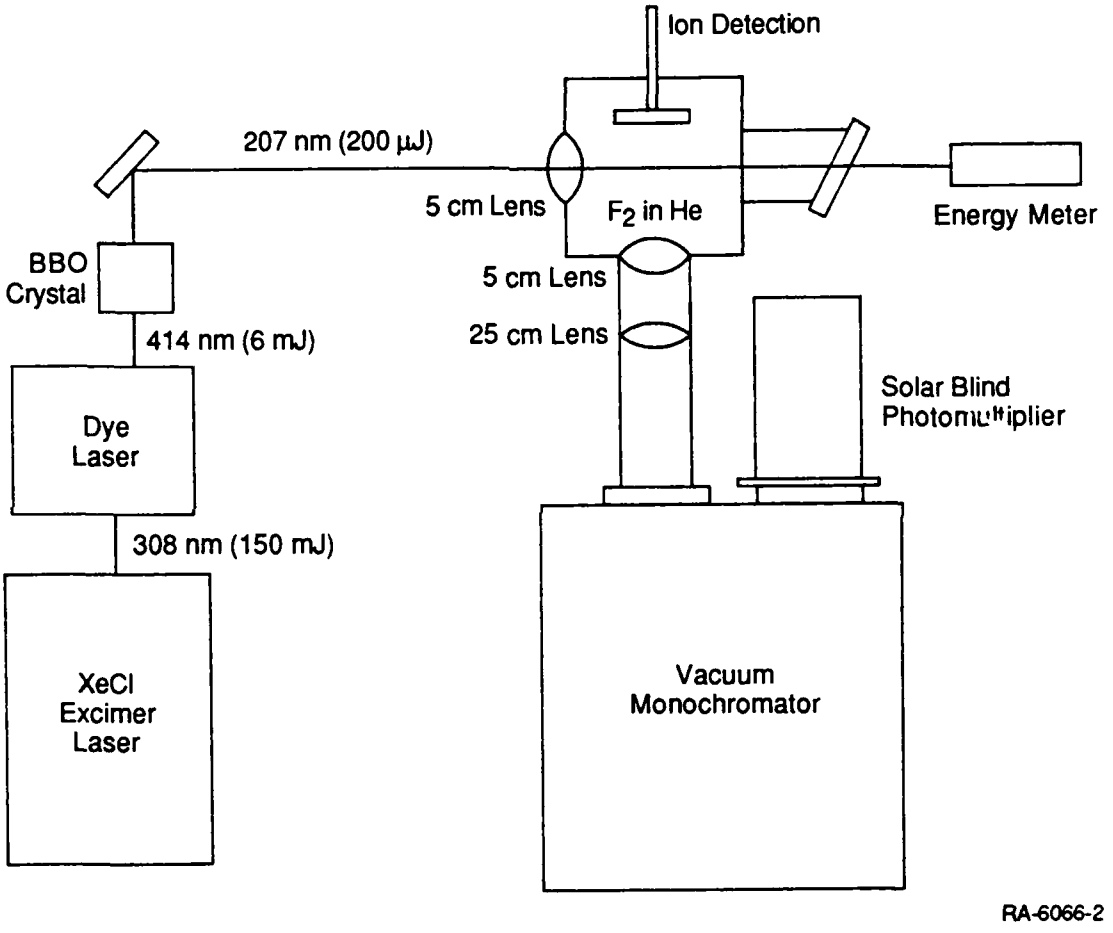

Figure 2. Experimental schematic for F_2 detection.

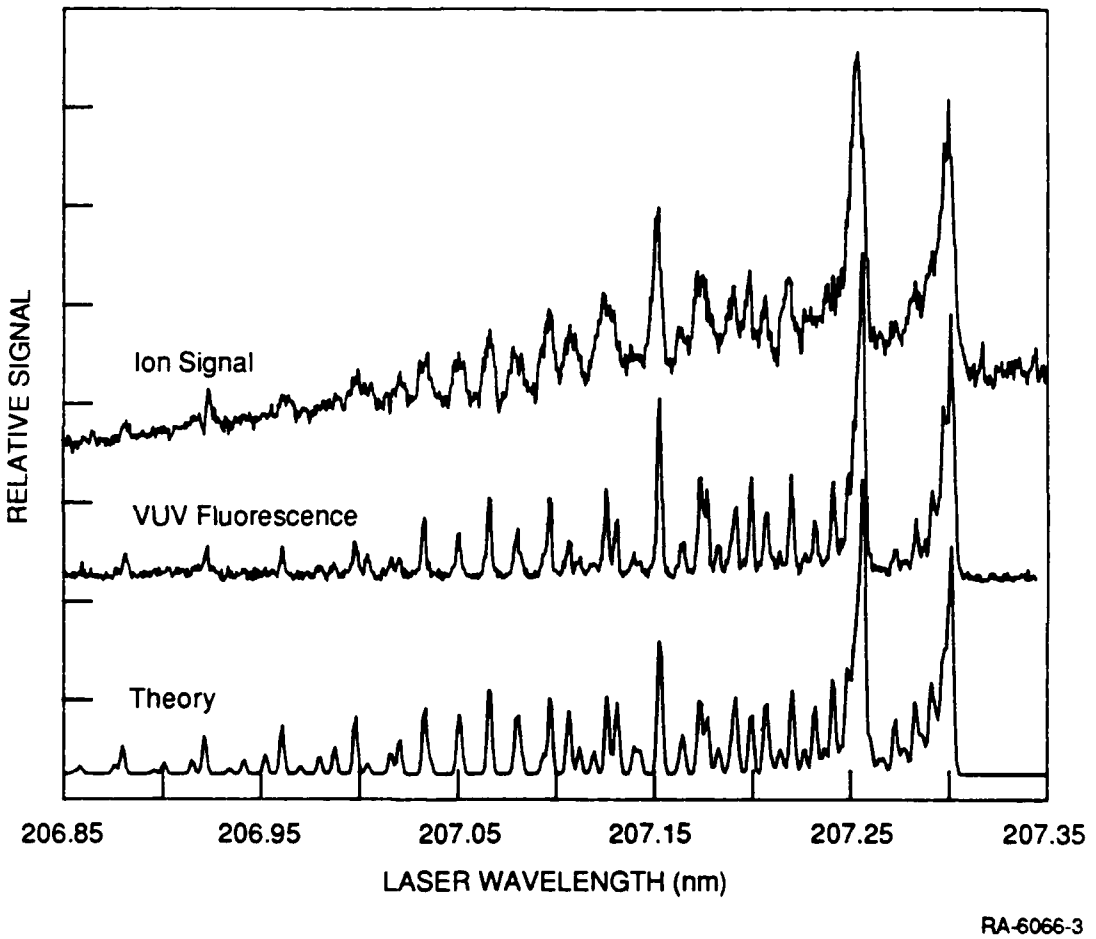

Figure 3. $F_2\ F^1\Pi_g\ (v' = 2) \leftarrow X^1\Sigma_g^+\ (v'' = 0)$ two-photon spectra.

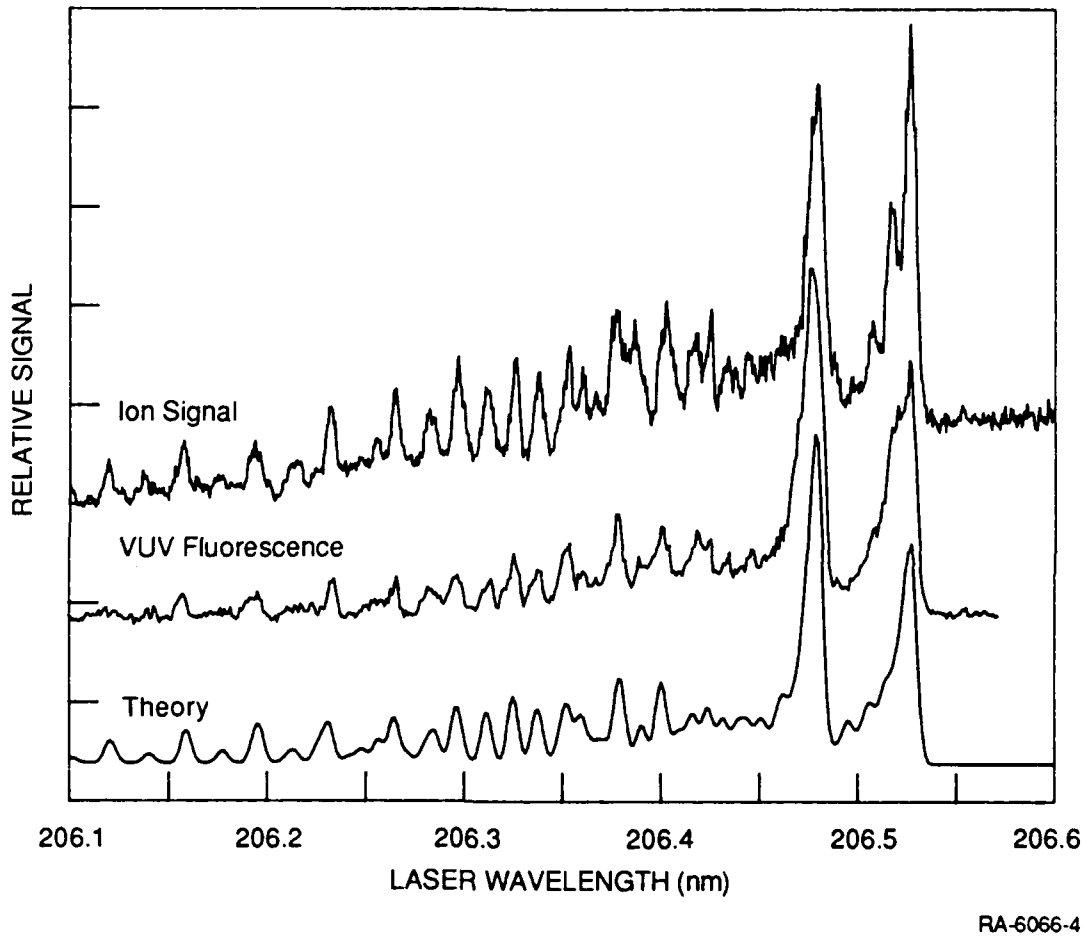

Figure 4. F_2 $F^3\Pi_g$ (v' = 3) ← $X^1\Sigma_g^+$ (v" = 0) two-photon spectra.

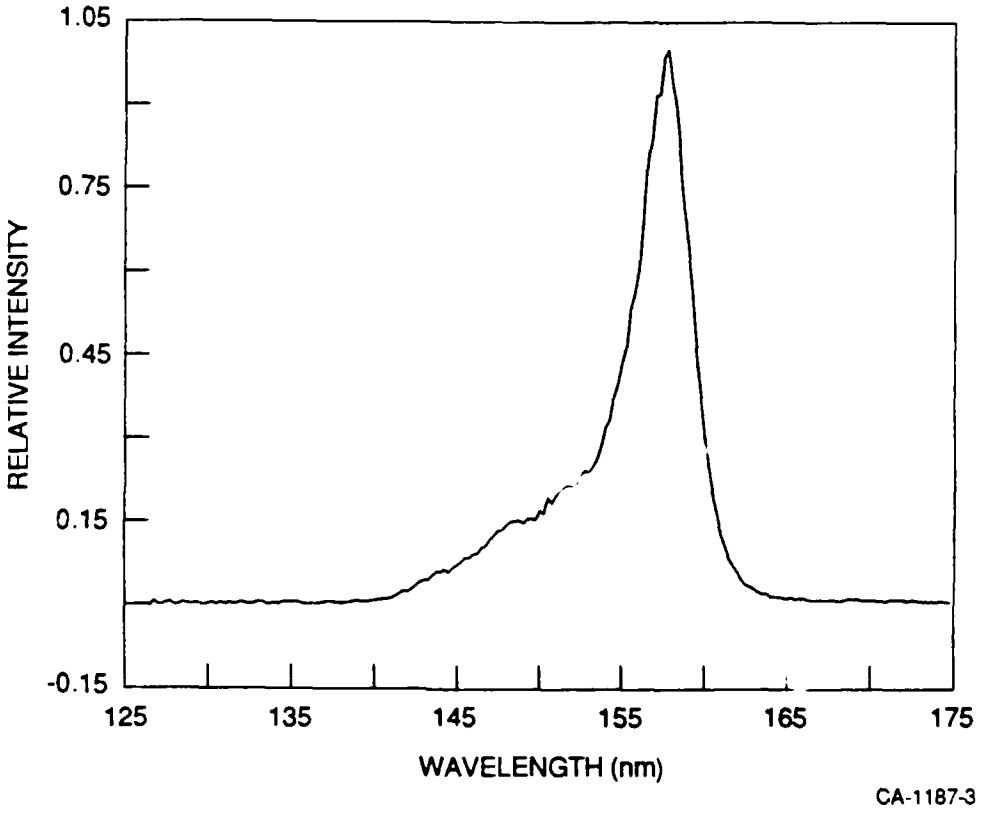

Figure 5. VUV emission on excitation of the F_2 $F^1\Pi_g$ (v' = 2) state.

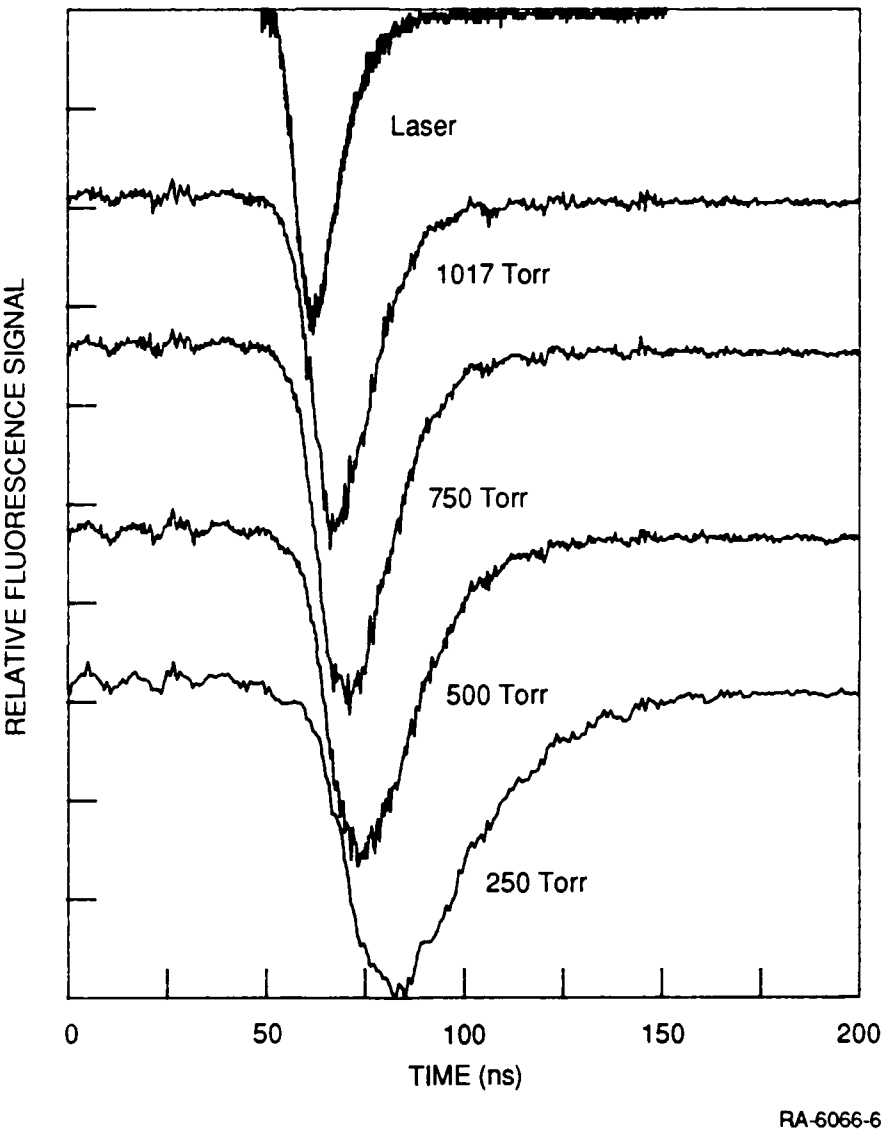

Figure 6. Pressure dependence of the F_2 $F^1\Pi_g$ (v' = 2) state fluorescence signal.

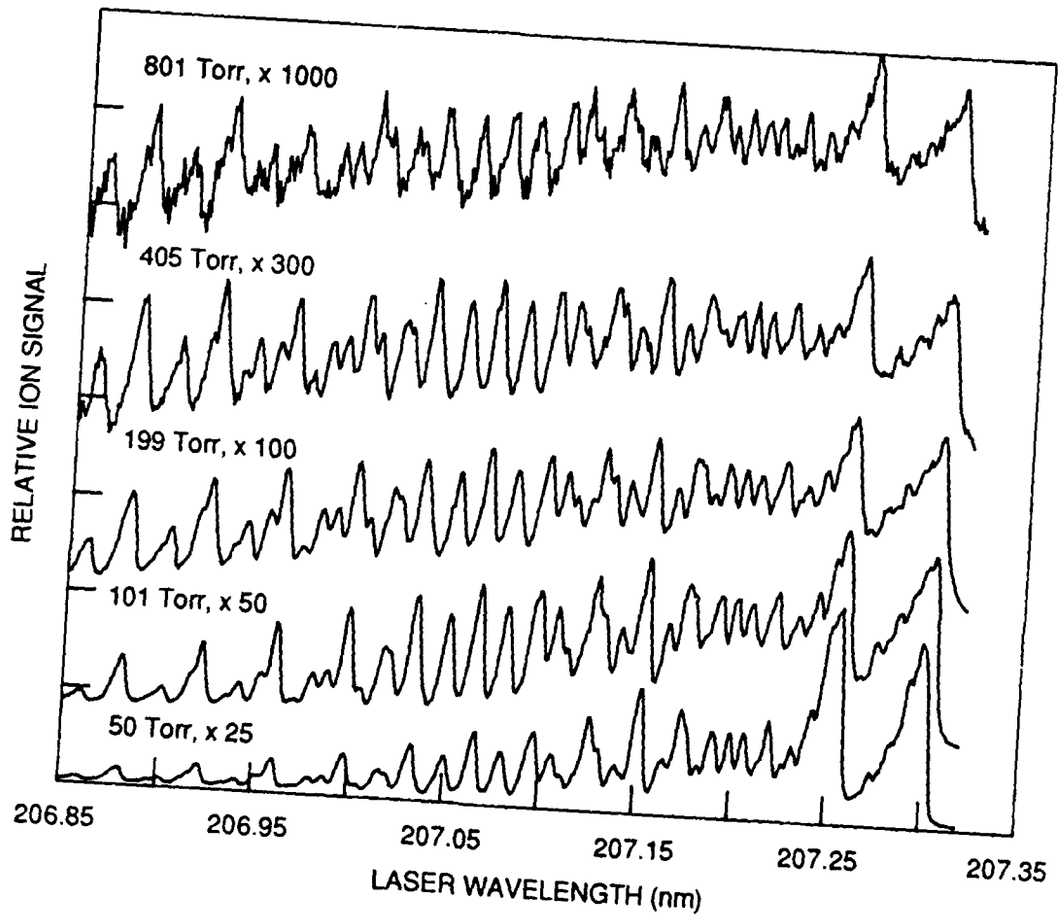

Figure 7. F_2 $F^1\Pi_g$ ($v' = 2$) $\leftarrow$ $X^1\Sigma_g^+$ ($v'' = 0$) MPI spectra as a function of pressure.